Optimal planning of self-healing multi-carriers energy systems considering integration of smart buildings and parking lots energy resources

Mehrdad Setayesh Nazar [a], Pourya Jafarpour [a], Miadreza Shafie-khah [b], João P.S. Catalão [c,*]

[a] *Shahid Beheshti University, Tehran, Iran*
[b] *School of Technology and Innovations, University of Vaasa, 65200, Vaasa, Finland*
[c] *Research Center for Systems and Technologies (SYSTEC), Advanced Production and Intelligent Systems Associate Laboratory (ARISE), Faculty of Engineering, University of Porto, 4200-465, Porto, Portugal*

A B S T R A C T

This paper presents a new framework for optimal planning of electrical, heating, and cooling distributed energy resources and networks considering smart buildings' contribution scenarios in normal and external shock conditions. The main contribution of this paper is that the impacts of smart buildings' commitment scenarios on the planning of electrical, heating, and cooling systems are explored. The proposed iterative four-stage optimization framework is another contribution of this paper, which utilizes a self-healing performance index to assess the level of resiliency of the multi-carrier energy system. In the first stage, the optimal decision variables of planning are determined. Then, in the second stage, the smart buildings and parking lots contribution scenarios are explored. In the third stage, the optimal hourly scheduling of the energy system for the normal condition is performed considering the self-healing performance index. Finally, in the fourth stage, the optimization process determines the optimal scheduling of system resources and the switching status of electrical switches, heating, and cooling pipelines' control valves. The proposed method was successfully assessed for the 123-bus IEEE test system. The proposed framework reduced the expected values of aggregated system costs and energy not supplied costs by about 49.92% and 93.64%, respectively, concerning the custom planning exercise.

1. Introduction

The concept of self-healing of energy systems is highly utilized in the planning exercises of energy infrastructures based on the fact that the external shock of the energy systems can interrupt the services, reduce social welfare, and decrease the consumers' comfort [1]. A Self-healing Multi-Carrier Energy System (SMCES) should be designed in a way that the worst-case external shock can be tolerated; the system can recover from the extreme contingencies, and carry on with continuous steady-state operation [2]. The external shocks can be natural cataclysmic events, kinetic attacks, and cyber-attacks [3]. The multi-carrier energy system may have Combined Cool, Heat, and Power (CCHP) units, gas-fired Distributed Generations (DGs), Absorption chillers (ACHs), Compression chillers (CCHs), PhotoVoltaic arrays (PV), Wind Turbines (WTs), Plug-in Hybrid Electrical Vehicle (PHEV) Parking lots (PLOTs), Electrical Energy Storages (ESSs), Cool Storage Systems (CSSs), Thermal energy Storage Systems (TSSs), and boilers [4]. Further, the consumer's smart building may have distributed energy resources that consist of

energy storage, DGs, Combined Heat and Power (CHP) generation units, intermittent power generation facilities, plug-in electric vehicles, and smart appliances.

The Optimal Self-healing multi-carrier Energy System Planning (OSESP) problem determines the multi-carrier energy resources' location, capacity, and time of installation. The self-healing planning of a multi-carrier energy system has different sources of uncertainties that consist of multi-carrier energy demands, intermittent electricity generations, smart buildings and parking lots commitment scenarios, external shocks location and intensity, and electricity market prices. The OSESP is an important process from the social welfare, stability, and energy-economic points of view. However, there are a few types of research on the OSESP procedure in the recent literature. As shown in Table 1, the papers can be categorized into the following categories.

The first category determined the specification of facilities and modeled the external shock impacts on the electrical system. Ref. [4] assessed a three-stage expansion-planning algorithm for electrical distribution systems considering the non-utility capacity withholding in

---

Table 1
Comparison of proposed DERNEP with other papers.

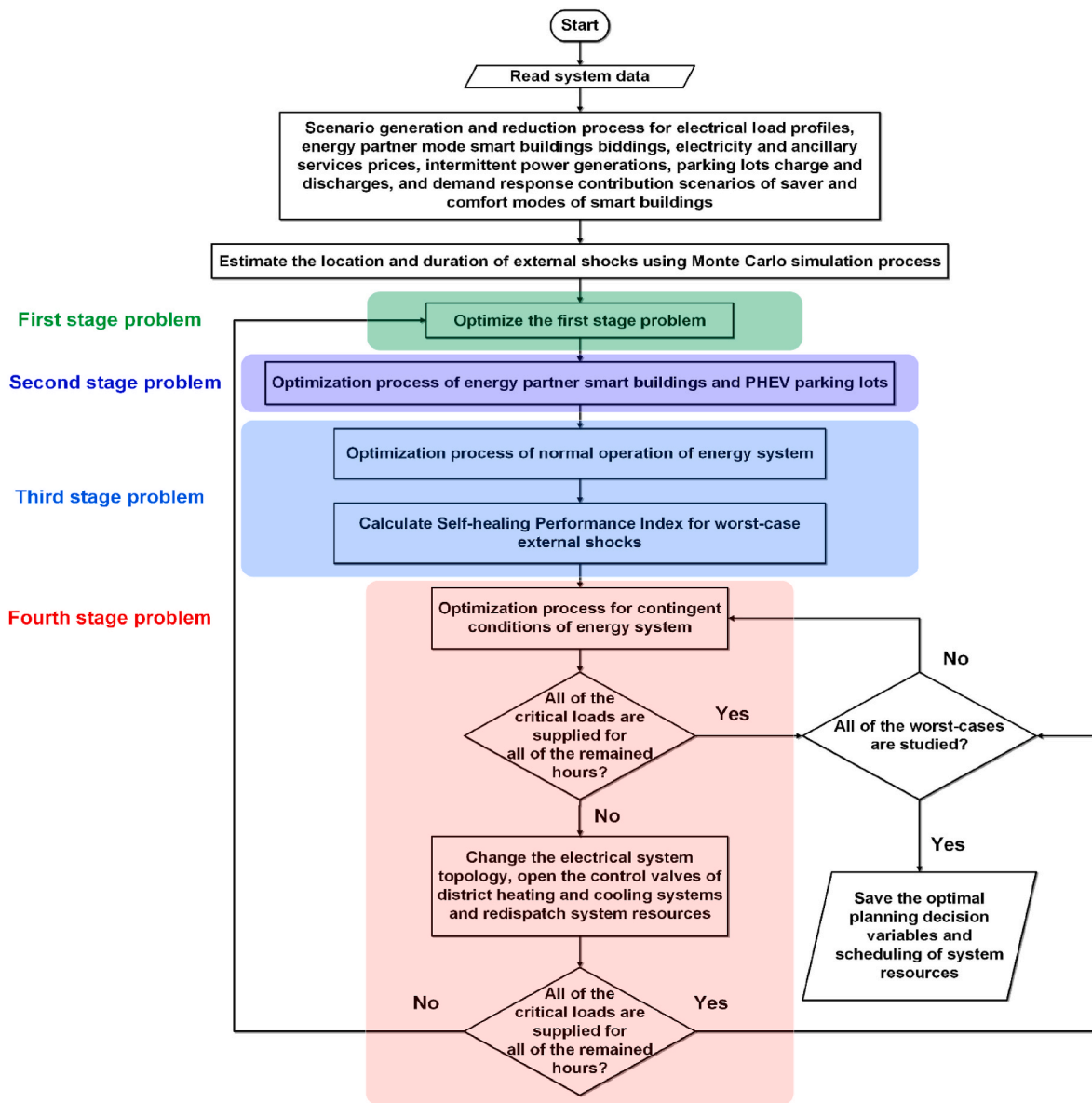| References		4	5	6	7	8	9	10	11	12	13	14	15	16	17	18	19	20	21	22	23	24	25	Proposed model
Categorization of smart homes modes		×	×	×	×	×	×	×	×	×	×	×	×	×	×	×	×	×	×	×	×	×	×	✓
Ancillary services of smart homes		×	×	×	×	×	×	×	×	×	×	×	×	×	×	×	×	×	×	×	×	×	×	✓
Ancillary services of parking lots		×	×	×	×	×	×	×	×	×	×	×	×	×	×	×	×	×	×	×	×	×	×	✓
Self-healing Performance Index		×	×	×	×	×	×	×	×	×	×	×	×	×	×	×	×	×	×	×	×	×	×	✓
Corrective District Heating and Cooling Valve Control		×	×	×	×	×	×	×	×	×	×	×	×	×	×	×	×	×	×	×	×	×	×	✓
Sectionalizing Electrical System into Multi-Microgrids		×	×	×	×	×	×	×	×	×	×	×	×	×	×	×	×	×	×	×	×	×	×	✓
Method	**MILP**	×	✓	✓	×	×	×	✓	✓	×	✓	×	×	×	×	×	×	✓	×	✓	×	✓	×	×
	MINLP	×	×	×	×	×	×	×	×	×	×	×	×	×	✓	×	×	×	×	×	×	×	×	×
	Heuristic	✓	×	×	✓	✓	×	×	×	✓	×	✓	✓	✓	×	✓	✓	✓	×	✓	×	✓	×	×
	Deterministic	×	×	×	✓	✓	×	×	×	✓	×	✓	×	✓	×	×	×	×	×	×	×	×	×	×
	Stochastic	×	✓	✓	×	×	✓	×	✓	×	✓	×	✓	×	×	×	×	×	×	×	×	✓	✓	✓
Objective Function	**Revenue**	×	×	×	×	×	×	×	×	×	×	×	✓	✓	×	×	×	×	×	×	×	✓	✓	✓
	Gen. Cost	✓	✓	✓	✓	×	✓	×	×	×	✓	✓	✓	✓	✓	✓	✓	✓	✓	✓	✓	✓	✓	✓
	Storage Cost	✓	✓	✓	×	×	✓	×	×	×	×	×	✓	✓	✓	✓	×	✓	×	✓	✓	✓	×	✓
	Secu. Costs	✓	✓	×	✓	×	×	✓	✓	✓	✓	✓	✓	✓	×	×	×	×	×	×	×	×	×	✓
	PHEV cost	✓	×	×	×	×	×	×	×	×	×	×	×	×	×	×	×	×	×	×	×	×	×	✓
	DRP costs	✓	×	×	×	×	×	×	×	×	×	✓	✓	✓	✓	✓	×	✓	×	×	×	✓	✓	✓
	WT	✓	×	✓	×	×	×	×	×	×	×	✓	✓	×	✓	×	✓	✓	✓	✓	×	×	✓	✓
	PV	✓		✓	×	×	×	×	×	×	×	✓	✓	✓	×	✓	×	✓	✓	✓	✓	×	✓	✓
	Smart Building	×	×	×	×	×	×	×	×	×	×	×	×	×	×	×	×	×	×	×	×	×	×	✓
	Parking Lots	×	×	×	×	×	×	×	×	×	×	×	×	×	×	×	×	×	×	×	×	×	×	✓
Storage Systems	**EES**	✓	×	✓	×	×	×	×	×	×	×	✓	✓	✓	×	×	✓	✓	×	×	×	×	×	✓
	TSS	×	×	×	×	×	×	×	×	×	×	✓	✓	×	×	×	×	×	×	×	×	×	×	✓
	CSS	×	×	×	×	×	×	×	×	×	×	×	×	×	✓	×	×	×	×	×	×	×	×	✓
Uncertainty Model	**PHEV**	✓	×	×	×	×	×	×	×	×	×	×	×	×	×	×	×	×	×	×	×	×	×	✓
	DRP	×	×	×	×	×	×	×	×	×	×	×	×	×	×	×	×	×	×	×	×	×	×	✓
	Market price	✓	×	×	×	×	×	×	×	×	×	×	×	×	×	×	×	×	×	×	×	×	×	✓
	Smart Building	×	×	×	×	×	×	×	×	×	×	×	×	×	×	×	×	×	×	×	×	×	×	✓
	Parking Lots	×	×	×	×	×	×	×	×	×	×	×	×	×	×	×	×	×	×	×	×	×	×	✓
	External Shock	✓	×	✓	✓	✓	×	×	✓	✓	✓	×	×	×	×	×	×	×	×	×	×	×	×	✓
	Loads	×	×	×	✓	×	×	✓	×	×	×	×	✓	×	×	×	×	×	×	×	×	×	×	✓
	Inter. electricity generation	✓	×	✓	✓	×	✓	✓	×	×	×	×	✓	×	×	×	×	×	×	×	×	×	×	✓

Fig. 1. The overall flowchart of the proposed procedure.

extreme contingency conditions. The first stage problem minimized the investment and operational costs of the system for planning horizon. The second stage problem explored the non-utility electricity generation facilities' bidding strategy impacts on the availability of energy resources. Finally, the third stage process determined the optimal commitment of system and non-utility energy resources. The algorithm reduced the investment and operating costs of the 123-bus system by about 23.74%, in comparison with the custom expansion planning exercise. However, the method did not model multi-carrier energy systems, smart building operating modes, and the impacts of smart buildings' commitment scenarios on the planning problem. Ref. [5] presented an approach to finding the best configuration of a microgrid-based electrical distribution system, which determined the optimal connection of the microgrid to the system's buses. Three optimization processes were utilized to determine the optimal topology of distribution for the connection of microgrids. The optimization processes were stationary heuristic method, time-dependent heuristic algorithm, and mixed-integer linear programming. The first and second optimization algorithm considered the worst-case scenario and optimal commitment of energy resources considering discrete time domains,

respectively. The mixed-integer linear programming maximized the critical load serving. The model did not consider smart homes' commitment processes in normal and external shock conditions. Ref. [6] proposed a stochastic two-stage optimization process to find the allocation and capacity of energy resource facilities and explored the system's operating conditions considering external shock. The first stage problem minimized the investment and operating costs. The second stage problem considered the grid connecting and island modes, which minimized the operating costs for grid connecting mode and maximized the volume of served load for island operating conditions. The paper did not explore the expansion planning of multi-carrier energy systems and smart buildings contributions. Ref. [7] introduced an index to determine the resiliency level of the system and utilized the concept of microgrids' formation in external shock operating conditions. The model utilized graph theory to determine the sets of formable microgrids, which were considered as the available candidates to connect to the distribution system. The switching process was considered to find the best reconfiguration options for the system considering the microgrids connection alternatives. Finally, the impacts of external shocks on the system were analyzed. However, the model did not consider the smart homes'
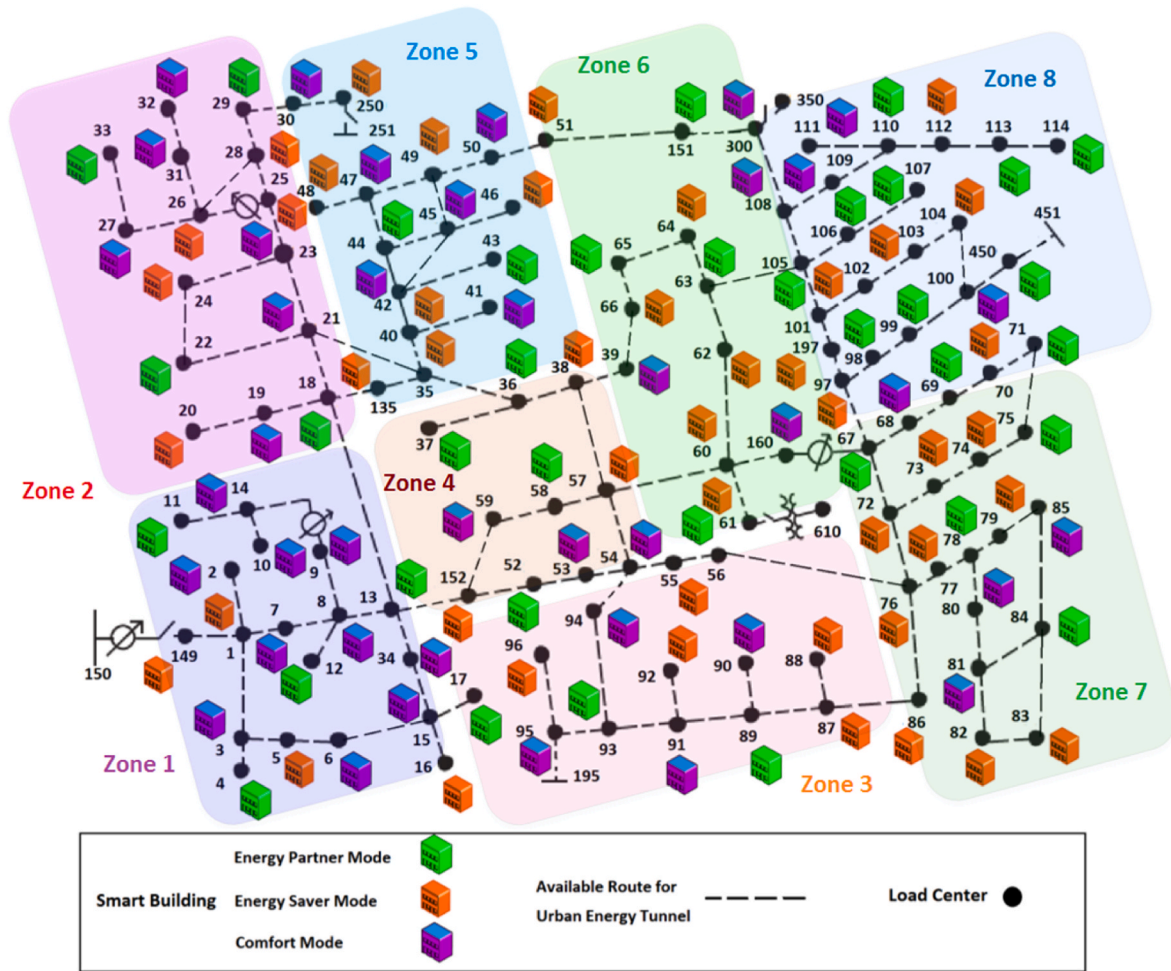
Fig. 2. The modified 123-bus IEEE test system.

Table 2
The scenario generation and reduction scenarios.

System parameter	Value
Number of solar irradiation scenarios	1000
Number of wind turbine power generation scenarios	1000
Number of PHEVs scenarios	1000
Number of demand response scenarios	1000
Number of load and price scenarios	1000
Number of energy partner smart buildings bidding scenarios	1000
Number of solar irradiation reduced scenarios	10
Number of wind turbine power generation reduced scenarios	10
Number of PHEVs contribution reduced scenarios	10
Number of demand response contribution reduced scenarios	10
Number of load and price-reduced scenarios	10
Number of energy partner smart buildings bidding scenarios	10

Table 3
The characteristics of distributed generation units [16].

Electrical power output (kW)	Fuel consumption (m^3/kWh)	Operating and maintenance costs (MUs/kWh)	Investment costs (MUs)*10^3
150	0.131	18.32	86.6347
200	0.218	19.69	94.3921

Table 4
The characteristics of combined heat and power generation units [16].

Electrical power output (kW)	Fuel consumption (m^3/kWh)	Operating and maintenance costs (MUs/kWh)	Investment costs (MUs)*10^3
294	0.266	32.2	189.8505
330	0.259	31.8	213.0975
335	0.269	31.9	212.3481
418	0.259	32.7	263.4197
435	0.252	32.4	270.2621
540	0.277	33.1	334.5300
559	0.259	32.8	346.3005

Table 5
The characteristics of boilers [16,32].

Boiler capacity	Heating surface (m^2)	Gas consumption (m^3/hr)	Investment costs (MUs/W)
1000 (kW)	50	98	370
1250 (kW)	60	124	441
1500 (kW)	70	193	511
2000 (kW)	93	243	418
3000 (kW)	118	385	455

commitment impacts on the planning process of the multi-carrier energy system. Ref. [8] proposed the structural resilience concept and determined the operating condition of the electrical system in the worst-case contingencies. The model utilized two resilience perspectives to assess the condition of the system after the shock impacts: the structural perspective that explored the connectivity of the system and the service perspective that evaluated the volume of energy delivered. The

Table 6
The input parameters of the simulation process [13].

	Parameters
Photovoltaic system	Investment cost= 1.48E+5 (MMUs/m^2 .MW), Lifetime=25(years), Maintenance cost=5.55E+01 (MMUs/MWh)
Wind turbine	3.5(kW) @ 250 (rpm), Cut-in speed= 3(m/s), Total length=3 (m), Type: Up-wind horizontal rotor, noise: 37 dB(A) from 60 (m) with a wind speed 8 (m/s) , Investment cost =2.4E+03 (MMUs), Maintenance cost =3.7E+04 (MUs/MWh)
Absorption chiller	Investment cost =4.0811E+03 (MMUs), Operating cost=6.4195E+03 (MMUs/MWh), Maintenance cost=3.81E+04 (MUs/MWh), COP=0.81, Lifetime=25 (years)
Compression chiller	Investment cost =4.218E+03 (MMUs), Operating cost =4.736E+03 (MMUs/MWh), Maintenance cost =3.77E+04 (MUs/MWh), COP=4, Lifetime=25(years)
Electrical storage system	Modules capacity= 100 (kW), Type: Lead-acid battery, Efficiency=0.75, Investment cost=11.285E+03 (MMUs/MWh), Operating and maintenance costs=5.55E+02 (MMUs/MWh), Lifetime=3500 (cycle number)
Thermal energy storage system	TSS modules capacity= 100 kW, TSS type (hot water storage) Investment cost= 5.98E+02 (MMUs/MWh) , Operating and maintenance costs =1.6E+01 (MMUs/MWh), Lifetime=25(years)
Cool storage system	CSS modules capacity= 100 kW, Maintenance cost (CSS)=30 MUs/kWh , CSS type (ice storage), Investment cost= 5.55E+02 (MMUs/MWh) , Operating and maintenance costs =1.2E+01 (MMUs/MWh), Lifetime=25(years)
Natural gas fuel price	44 MU/kWh
PHEV	Minimum PHEVs energy = 4 kWh, Maximum PHEVs energy = 18 kWh
District heating and cooling network	District heating fixed investment cost=2.59 (MMUs/m. MW), District heating length dependent investment costs=1.221E+01 (MMUs/m), District cooling fixed investment cost =2.59 (MMUs/m.MW), District cooling length dependent investment costs =1.221E+01 (MMUs/m), District heating loss=18% heating transmission, District cooling loss= 7% cooling transmission
Electrical feeder	Electrical feeder fixed investment cost=143267 (MUs/kW), Electrical feeder length dependent investment costs= 32641 (MUs/m)

Table 7
The electrical, heating, and cooling load interruption costs [16].

Parameter	Price
Average electrical load interruption costs zone (MMUs/MWh)	0.40
Average cooling load interruption costs zone (MMUs/MWh)	0.17
Average heating load interruption costs zone (MMUs/MWh)	0.24

structural resilience criteria determined the capacity of the distribution system to stay connected after external shocks. The service resilience criteria explored the volume of power delivered after external shock. However, the model did not consider the multi-carrier energy system planning and smart buildings' operating processes. Ref. [9] assessed a two-stage optimization algorithm to plan the system and coordinate the energy resources of a microgrid-based distribution system in the worst-case contingency. The first stage problem utilized a mixed-integer linear programming approach to find the optimal decision variables of the investment problem. The second stage problem carried out the market simulation process using the nodal-pricing mechanism considering the Nash equilibrium model for finding the energy transactions of microgrids. The case study was performed for three islands on the west coast of Norway. The model did not model the planning process of the multi-carrier energy system and the smart homes commitment strategies. Ref. [10] introduced an algorithm for the restoration of loads in

contingency conditions considering demand response programs. The mixed-integer linear programming process was utilized for optimizing the problem. The objective function maximized the served critical loads considering the network and microgrids' constraints. An urban electrical system and the 33-bus IEEE test system were used to assess the method. The proposed model did not consider the smart homes' commitment modes and their commitments in contingency conditions of a multi-carrier energy system. Ref. [11] evaluated an algorithm for switching device allocation to enhance the resiliency level of system. A two-stage mixed-integer linear programming optimization process determined the impact of extreme weather conditions on the system and the resiliency index in the first and second stages, respectively. The model considered the N-1 and N-2 failure constraints scenarios in the optimization process. The switching devices' allocation problem minimized the interrupted loads for the failure scenarios. The process did not assess the smart buildings operating modes' impacts on the OSESP problem. Ref. [12] assessed a multi-level resilient model to determine the best preventive/corrective plans against external shocks. In the first stage, the preventive decisions were determined; in the second stage, the worst-case operating conditions were assessed, and in the third stage, the resilient operational scheduling was optimized. The optimization process utilized a mixed-integer linear programming process. The proposed model was assessed by the 94-bus and 33-bus systems. The model did not evaluate the operational scheduling of smart homes in external shock conditions. Ref. [13] proposed the resilient planning of electrical systems considering the N–K contingency planning process. A two-stage robust optimization procedure was used and the dynamics of uncertain natural disasters were modeled. The model determined the optimal coordination of hardening processes; meanwhile, allocated the electricity generation facilities to minimize the unserved loads. The 123-bus and 33-bus test systems were considered for case studies. However, the algorithm did not model the multi-carrier energy system and smart buildings' commitments. Ref. [14] proposed self-healing planning and operation of the electrical distribution system. The model determined the optimal control actions for contingency conditions of the system. The method considered the energy loss, supplied load, and the number of unfaulted zones as objective functions. The decision variables of the planning process were the size and allocation of energy resources; meanwhile, the decision variables of the operating problem were the outputs of energy resources, the status of switches, and the volume of shed loads. The results showed that the proposed method reduced the probable shed load of the 123-bus test system. However, the smart buildings' commitment scenarios and their operating modes were not modeled in the problem.

The second category of papers only optimized the multi-carrier energy system planning for normal operating conditions and did not consider the external shock impacts on the system planning. The formulations of these papers were assessed to consider their proposed methods for developing the present paper framework.

Ref. [15] introduced a three-stage optimization method for distributed energy resource and network planning of industrial microgrids considering the transaction of electricity between microgrids. In the first stage, the characteristics and allocation of system resources were determined considering the uncertainties of the input parameters. In the second stage, the feasibility of electricity transactions between microgrids and optimal scheduling of resources were determined. Finally, in the third stage, the contingent conditions of the system were explored. Ref. [16] presented an iterative bi-level optimization framework for the optimal planning of distributed energy resources and networks of CCHP-based microgrids. The model minimized the aggregated operating and investment costs; meanwhile, maximized the electrical system reliability. The method was assessed for a real building complex and different planning scenarios were considered to evaluate the impacts of energy resource configurations and operational scheduling on the system's costs. Refs. [15,16] did not consider the optimal switching of district heating and cooling control valves, smart homes commitments,
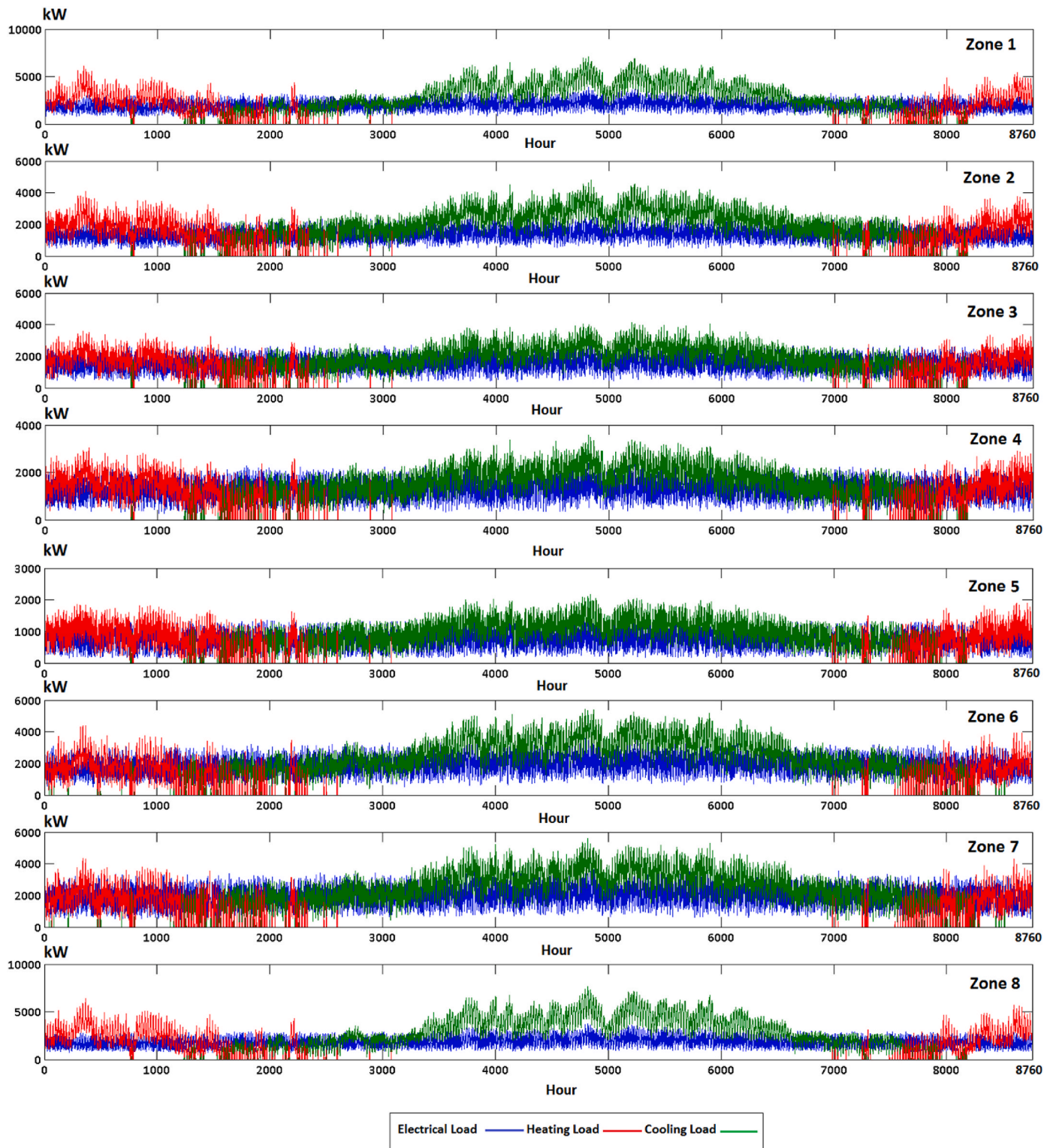
Fig. 3. The estimated values of electrical, heating, and cooling load profiles for the horizon year (2028).

and parking lots' contributions. Ref. [17] determined the sizing and configuration of combined cool, heat, and power facilities using a mixed-integer non-linear programming model. The model considered photovoltaic and storage systems to reduce CO_2 emissions. The objective function minimized the investment and operating costs, emission of pollutants, and energy purchased costs. The minimum energy bill and low carbon emission planning scenarios were considered. The method was assessed for a pilot district in China. Ref. [18] proposed a multi-criteria optimization model considering energy, economic, and environmental parameters. The optimization model utilized the analytic hierarchy method to optimize the objective function weighting factors. Different feed-in tariffs were assessed for Sino-Singapore. However, Refs. [17,18] did not model the optimal dispatch of system resources in external shock conditions. Further, Refs [17,18] did not control the district heating and cooling pipelines' control valves. Ref. [19] considered the operating costs, energy rate, and pollutant emission as objective
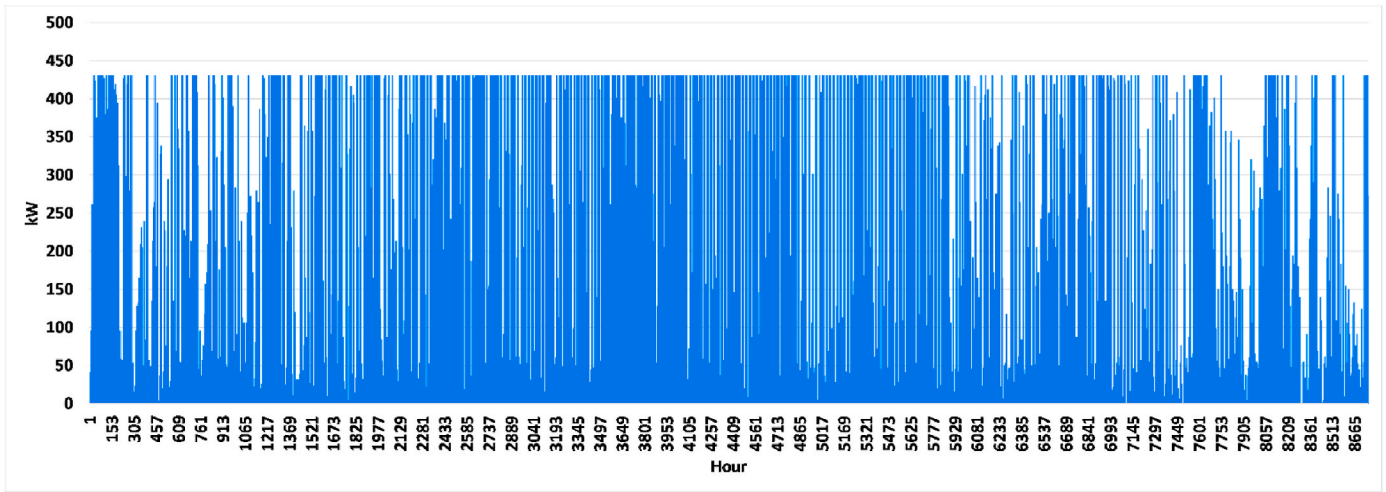
Fig. 4. The forecasted electricity generation of photovoltaic arrays for the final year of planning.
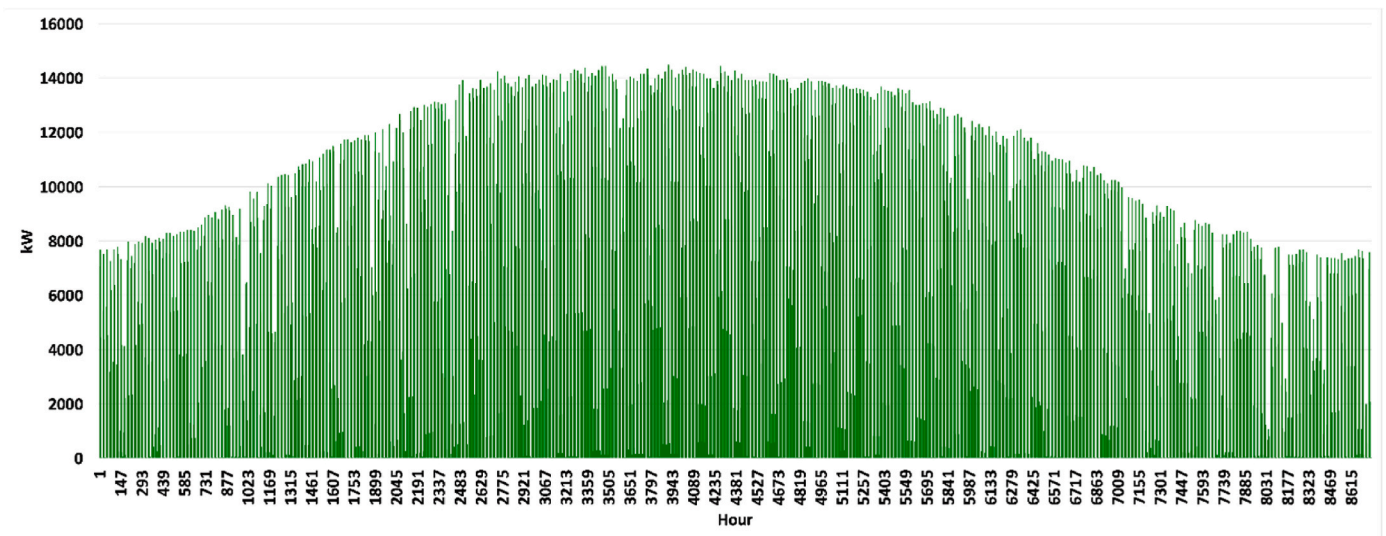
Fig. 5. The forecasted electricity generation of wind turbines for the final year of planning.

functions. The model determined the optimal design and operational planning of CCHP-based systems. An entropy weight method was used to solve the problem. Multiple operating scenarios were assessed in the model and different sensitivity analyses were performed. Ref. [20] evaluated an optimization process that utilized a fuzzy selection method, in which energetic, economic, and environmental criteria were considered as optimization objective functions. The simulation results revealed that the CCHP-based system reduced the system costs and pollutant emissions. However, the simulation results showed that these systems had no economic merits for residential customers. Refs. [19,20] did not model smart homes' modes of operation, switching of energy system's electrical switches and heating and cooling control valves, and resilient operation of the system. Ref. [21] considered the planning of microgrids that utilized distributed energy resources. The model minimized operating and investment costs in the first level problem; meanwhile, maximized the reliability of the system and profits of the microgrid owner in the second level problem. The Interval Linear Programming (ILP) optimization process was utilized to model the stochastic behavior of intermittent energy resources. The outputs of the ILP optimization algorithm were compared with the robust optimization process and the authors concluded that the robust optimization model caused over-investment solutions. Ref [22] introduced a two-level

mixed-integer non-linear optimization process. The size and location of energy resources were optimized considering the distributed energy resources' operational scheduling impacts on the planning procedure. The intermittent energy generation facilities and energy storage facilities were modeled. The model was solved using a hybrid co-evolutionary cultural algorithm. However, Refs. [21,22] did not assess the smart homes contribution scenarios and switching process of control valves in the external shock conditions. Ref. [23] evaluated a mixed-integer linear programming optimization process to find the optimal configuration of energy conversion technologies for a district energy system. The optimal mix of facilities and technologies was determined and the emissions of pollutants were minimized. Ref. [24] minimized the operating and investment costs of a CHP-based system using a multi-objective mixed-integer linear optimization process. The model considered the gas turbine and combustion engine systems as electricity generation facilities. The process was assessed for the city of Arenzani in Italy. The emission pollutants, capital, and operating costs were minimized using the proposed method. Ref. [25] assessed a model to minimize the planning costs of distributed energy resource systems using mixed-integer linear optimization. The method considered tariffs and climate constraints, and the parameters of district heating and distributed energy resource facilities were determined. Refs. [23–25]

Table 8
Final optimization process results.

Scenario	1	1	2	2	3	3	5	5
Year	1	5	1	5	1	5	1	5
DGs (kW)								
Zone 1	3*200	4*200	2*200	3*200	150+200	150+200	2*200	2*200
Zone 2	2*200	5*200	2*200	3*200	150+200	150+200	2*200	2*200
Zone 3	2*200	4*200	2*200	3*200	150+200	150+200	2*200	2*200
Zone 4	2*200	4*200	2*200	2*200	2*200	2*200	2*200	2*200
Zone 5	2*200	3*200	2*200	2*200	200	200	2*200	2*200
Zone 6	2*200	3*200	2*200	2*200	200	200	2*200	2*200
Zone 7	2*200	2*200	2*200	2*200	200	200	200	200
Zone 8	2*200	2*200	2*200	2*200	200	200	200	200
CHPs (kW)								
Zone 1	-	-	1*582	1*582	1*582	1*582	1*435	1*435
Zone 2	-	-	1*435	1*435	1*435	1*435	1*330	1*330
Zone 3	-	-	1*418	1*418	1*418	1*418	1*330	1*330
Zone 4	-	-	1*335	1*335	1*335	1*335	1*250	1*250
Zone 5	-	-	1*200	1*200	1*200	1*200	1*180	1*180
Zone 6	-	-	1*335	1*335	1*335	1*335	1*294	1*294
Zone 7	-	-	1*335	1*335	1*335	1*335	1*294	1*294
Zone 8	-	-	1*559	1*559	1*559	1*559	1*418	1*418
Boilers (kW)								
Zone 1	1*3000	2*3000	1*3000	2*3000	1*3000	2*3000	2*2000	2*2000
Zone 2	2*2000	2*2000	2*2000	2*2000	2*2000	2*2000	2*1500	2*1500
Zone 3	2*2000	2*2000	2*2000	2*2000	2*2000	2*2000	2*1250	2*1250
Zone 4	1*3000	1*3000	1*3000	1*3000	1*3000	1*3000	2*1000	2*1000
Zone 5	1*2000	1*2000	1*2000	1*2000	1*2000	1*2000	1*1500	1*1500
Zone 6	2*2500	2*2500	2*2500	2*2500	2*2500	2*2500	2*1500	2*1500
Zone 7	2*2500	2*2500	2*2500	2*2500	2*2500	2*2500	2*1500	2*1500
Zone 8	1*3000	2*3000	1*3000	2*3000	1*3000	2*3000	2*2000	2*2000
ACH (kW)								
Zone 1	-	-	1*850	1*850	1*850	1*850	1*600	1*600
Zone 2	-	-	1*600	1*600	1*600	1*600	1*500	1*500
Zone 3	-	-	1*600	1*600	1*600	1*600	1*500	1*500
Zone 4	-	-	1*500	1*500	1*500	1*500	1*350	1*350
Zone 5	-	-	1*300	1*300	1*300	1*300	1*300	1*300
Zone 6	-	-	1*500	1*500	1*500	1*500	1*300	1*300
Zone 7	-	-	1*500	1*500	1*500	1*500	1*450	1*450
Zone 8	-	-	1*800	1*800	1*800	1*800	1*450	1*450
CCH (kW)								
Zone 1	2*3500	2*3500	1*3500	2*3500	1*3500	2*3500	2*2500	2*2500
Zone 2	2*2500	2*2500	2*2500	2*2500	2*2500	2*2500	2*1500	2*1500
Zone 3	2*2000	2*2000	1*2000	2*2000	1*2000	2*2000	2*1250	2*1250
Zone 4	2*2000	2*2000	1*2000	2*2000	1*2000	2*2000	1*2500	1*2500
Zone 5	2*1000	2*1000	2*1000	2*1000	2*1000	2*1000	1*1500	1*1500
Zone 6	2*2500	2*2500	1*2500	2*2500	1*2500	2*2500	2*2000	2*2000
Zone 7	2*2500	2*2500	1*2500	2*2500	1*2500	2*2500	2*1500	2*1500
Zone 8	2*3500	2*3500	1*3500	2*3500	1*3500	2*3500	1*3500	2*3500
PV (kW)								
Zone 1	2000	2000	2000	2000	2000	2000	2000	2000
Zone 2	2000	2000	2000	2000	2000	2000	2000	2000
Zone 3	2000	2000	2000	2000	2000	2000	2000	2000
Zone 4	2000	2000	2000	2000	2000	2000	2000	2000
Zone 5	2000	2000	2000	2000	2000	2000	2000	2000
Zone 6	1500	1500	1500	1500	1500	1500	1500	1500
Zone 7	1000	1000	1000	1000	1000	1000	1000	1000
Zone 8	2000	2000	2000	2000	2000	2000	2000	2000

Table 9
Final optimization results.

Scenario	1	1	2	2	3	3	5	5
Year	1	5	1	5	1	5	1	5
WT (kW)								
Zone 1	20*3.5	20*3.5	20*3.5	20*3.5	20*3.5	20*3.5	20*3.5	20*3.5
Zone 2	15*3.5	15*3.5	15*3.5	15*3.5	15*3.5	15*3.5	15*3.5	15*3.5
Zone 3	18*3.5	18*3.5	18*3.5	18*3.5	18*3.5	18*3.5	18*3.5	18*3.5
Zone 4	10*3.5	10*3.5	10*3.5	10*3.5	10*3.5	10*3.5	10*3.5	10*3.5
Zone 5	8*3.5	8*3.5	8*3.5	8*3.5	8*3.5	8*3.5	8*3.5	8*3.5
Zone 6	16*3.5	16*3.5	16*3.5	16*3.5	16*3.5	16*3.5	16*3.5	16*3.5
Zone 7	16*3.5	16*3.5	16*3.5	16*3.5	16*3.5	16*3.5	16*3.5	16*3.5
Zone 8	20*3.5	20*3.5	20*3.5	20*3.5	20*3.5	20*3.5	20*3.5	20*3.5
ESS (kWh)								
Zone 1	10*100	10*100	10*100	10*100	10*100	10*100	10*100	10*100
Zone 2	10*100	10*100	10*100	10*100	10*100	10*100	10*100	10*100
Zone 3	10*100	10*100	10*100	10*100	10*100	10*100	10*100	10*100
Zone 4	10*100	10*100	10*100	10*100	10*100	10*100	10*100	10*100
Zone 5	10*100	10*100	10*100	10*100	10*100	10*100	10*100	10*100
Zone 6	6*100	6*100	6*100	6*100	6*100	6*100	6*100	6*100
Zone 7	5*100	5*100	5*100	5*100	5*100	5*100	5*100	5*100
Zone 8	10*100	10*100	10*100	10*100	10*100	10*100	10*100	10*100
CSS (MWh)								
Zone 1	0	0	0	0	0	0	7	7
Zone 2	0	0	0	0	0	0	5	5
Zone 3	0	0	0	0	0	0	4	4
Zone 4	0	0	0	0	0	0	3.5	3.5
Zone 5	0	0	0	0	0	0	2	2
Zone 6	0	0	0	0	0	0	5.5	5.5
Zone 7	0	0	0	0	0	0	5.5	5.5
Zone 8	0	0	0	0	0	0	7.5	7.5
TSS (MWh)								
Zone 1	0	0	0	0	0	0	6	6
Zone 2	0	0	0	0	0	0	4	4
Zone 3	0	0	0	0	0	0	3.5	3.5
Zone 4	0	0	0	0	0	0	3	3
Zone 5	0	0	0	0	0	0	2	2
Zone 6	0	0	0	0	0	0	4.5	4.5
Zone 7	0	0	0	0	0	0	4.5	4.5
Zone 8	0	0	0	0	0	0	6.5	6.5

did not consider the impacts of parking lots and smart buildings on the self-healing planning of multi-carrier energy systems. Further, the switching process of electrical switches and district heating and cooling control valves were not modeled in Refs. [23–25].

As shown in Table 1, an integrated framework that models the smart buildings' heating and cooling energy carriers' injection into the SMCES district heating and cooling networks is less frequent in the literature and is not presented in the available literature before. In this paper, an integrated framework for the optimal planning of multi-carrier energy systems considering smart buildings' contribution scenarios is proposed. The proposed model optimally determines the allocation, capacity, and scheduling of the system's distributed energy resources considering the self-healing performance index and smart building energy generation/consumption scenarios.

The contributions of this paper are.

- The smart buildings operating scenarios are categorized into comfort, energy saver, and energy partner modes and the proposed model considers the electrical, heating, and cooling energy procurement scenarios from the smart buildings,

- The impacts of operating strategies of the smart buildings in the optimal planning of electrical, heating, and cooling networks are modeled and their optimal contribution scenarios in the external shock conditions are determined,
- A self-healing performance index is proposed to assess the self-healing process of the energy system in different operating conditions,
- The proposed algorithm determines the optimal scheduling of PHEV parking lots in normal and external shock conditions,
- The proposed method minimizes the impacts of the external shocks using electrical switches, and control of district heating and cooling control valves.

The paper is organized as follows: The formulation of the problem is introduced in Section II. In Section III, the solution algorithm is presented. In section IV, the simulation results are presented. Finally, the conclusions are included in Section V.
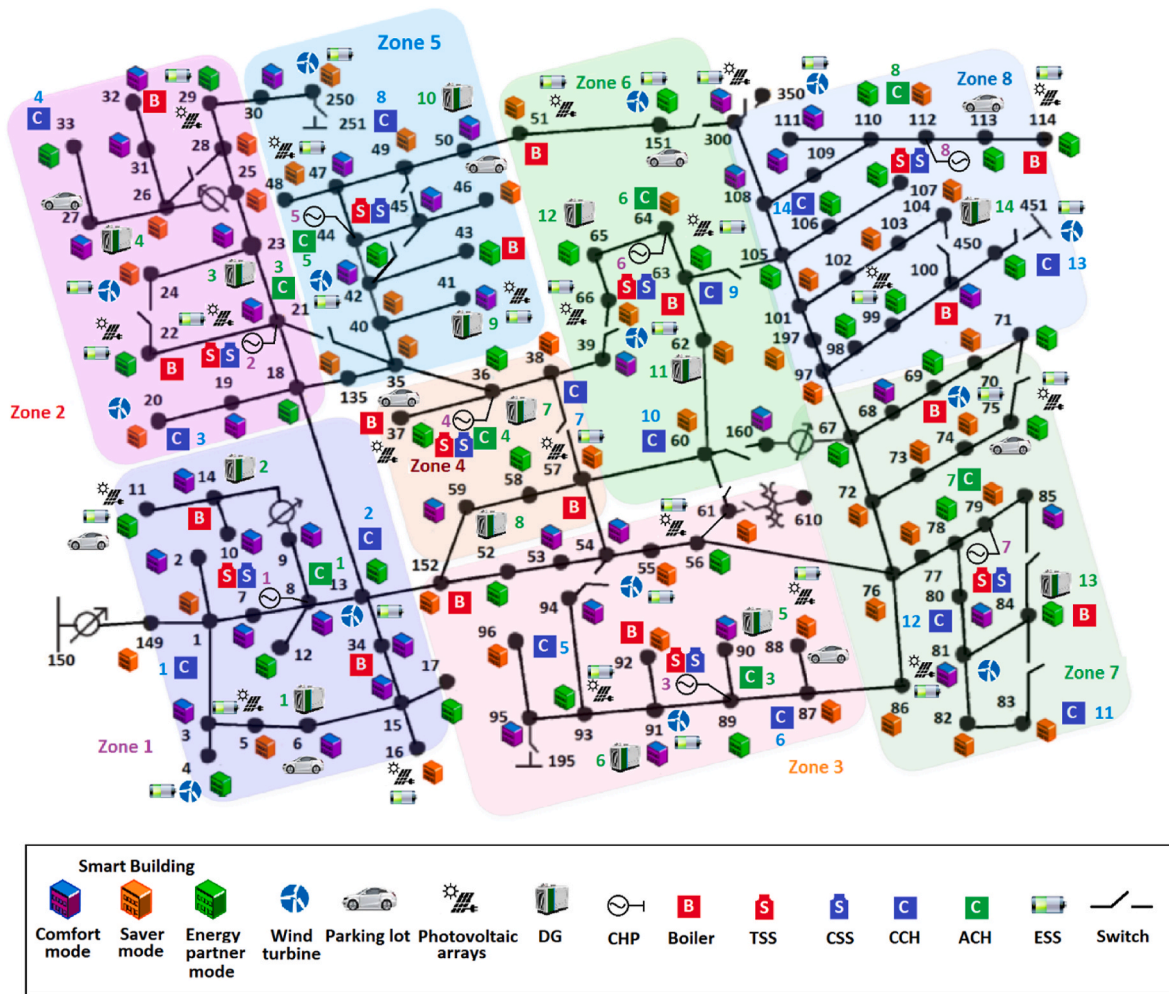
Fig. 6. The optimal topology of the system for the final year of planning and the fourth scenario.

2. Problem modeling and formulation

2.1. Smart building and parking lot modeling

A smart building may utilize small wind turbines, roof-mounted photovoltaic panels, CHPs, absorption chillers, compression chillers, boilers, energy storage facilities, plug-in electric vehicle parking, and smart appliances [26]. It is assumed that the Smart Building Energy Management System (SBEMS) continuously monitors the smart building loads, communicates with the SMCES dispatching center, receives control commands, and optimally commits the smart building's loads. Further, the smart building can purchase electricity, heating, and cooling energy carriers from the energy system through electrical, heating, and cooling networks, respectively. The smart buildings' electrical, heating, and cooling loads are categorized into deferrable, dispatchable, and non-dispatchable loads. The electrical, heating, and cooling deferrable loads cannot be interrupted during their operational time, and their operation times are fixed. Further, the time-of-use program can be performed for these loads to encourage the electrical, heating, and cooling loads to change the operation time of these loads to other times. The dispatchable electrical, heating, and cooling loads can be dispatched considering the consumers' comfort levels. It is assumed that the consumers' comfort levels are continuously monitored by the SBEMSs. The operating time of non-dispatchable electrical, heating, and cooling loads cannot be transferred to other times; these loads cannot be dispatched through the SBEMSS, and they can only be interrupted in external shock conditions.

Based on the above description, the smart buildings' operational modes are categorized into the following groups.

1) Comfort mode of multi-carrier energy consumption: the maximum value of the electrical, heating, and cooling loads of smart buildings are considered critical loads,
2) Saver mode of multi-carrier energy consumption: the smart building owner contributes to demand response programs to maximize his/her profits. The time-of-use process and direct load control are carried out for deferrable loads and dispatchable loads, respectively,
3) Energy Partner Smart Buildings (EPSBs): the smart building can deliver electrical, heating, and cooling energy carriers through the electrical network, district heating, and cooling networks, respectively [27].

It is assumed that the PHEV parking lot can purchase active and reactive power from the SMCES. Further, the parking lot can deliver active and reactive power and provide spinning reserves for the SMCES. The detailed models of PHEV parking lots are available in Refs. [1,28] and are not presented for the sake of space.

2.2. The proposed optimization framework

This paper proposes an iterative four-stage optimization framework to determine the optimal allocation, capacity, and specifications of electrical, heating, and cooling energy generation facilities and networks considering the smart building energy generation and

(a)

(b)
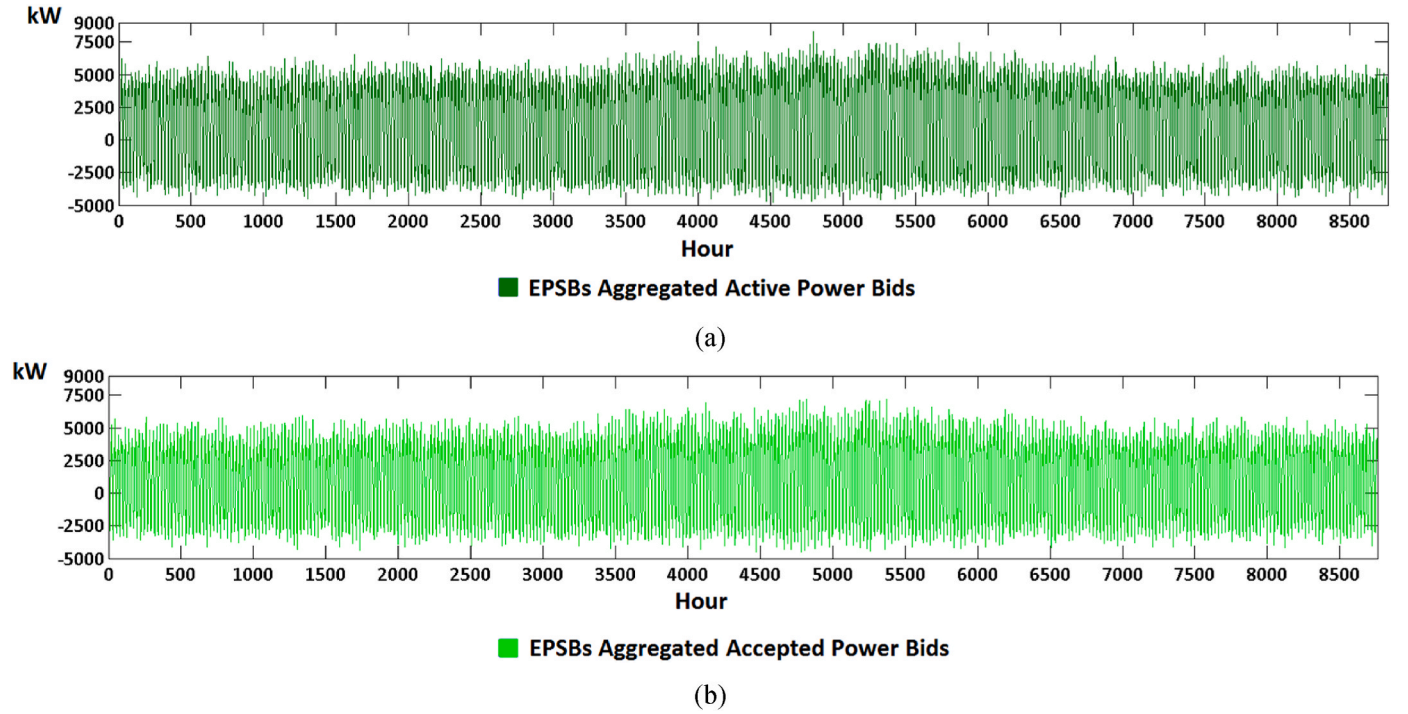
Fig. 7. The submitted values of EPSBs' active power (a), the accepted values of EPSBs' active power (b), the submitted values of EPSBs' reactive power (c), the accepted values of EPSBs' reactive power (d), the submitted values of EPSBs' spinning reserve (e), and the accepted values of EPSBs' spinning reserve (f) of distributed generation for the final year of planning and the third scenario.

consumption scenarios. The optimization process is decomposed into four stages. The first stage problem determines the optimal planning decision variables of the SMCES for the horizon year of planning. Then, in the second stage, the contribution scenarios of smart buildings and parking lots are explored. Then, in the third stage, the OSESP determines the optimal hourly optimal scheduling of distributed energy resources in normal conditions. Finally, in the fourth stage problem, the OSESP investigates the impacts of external shocks on the energy systems, optimizes the scheduling of system resources, switches the electrical switches, and performs the ON/OFF control of heating and cooling control valves in the external shocks.

2.3. First stage problem formulation

The first stage of OSESP minimizes the aggregated investment and operating costs for the planning horizon and the objective function of this stage can be written as (1):

$$
Min\ \mathfrak{M} = \sum_{NY}\sum_{NZ}\left(
\begin{array}{c}
\vartheta\cdot\left(\displaystyle\sum_{Xsite}\sum_{Xtype}\psi^X\cdot\left(C^X_{Invest}+\sum_{Xotime}\tau_X\cdot C^X_{Op}\right)\right)\\[2ex]
+\vartheta\cdot\left(\displaystyle\sum_{Ysite}\sum_{Ytype}\psi^Y\cdot\left(C^Y_{Cap}+L_X\cdot C^Y_{Length}\right)\right)\\[2ex]
\left(
\begin{array}{c}
\displaystyle\sum_{NSC}ENSC^M+\sum_{NSOS}prob\cdot C^N_{Purchase}+\sum_{NSOS}prob\cdot C^{N'}_{Purchase}\\[2ex]
-\displaystyle\sum_{NSOS}prob\cdot B^N_{Sell}+\\[2ex]
\displaystyle\sum_{NSOS}prob\cdot C^M_{DRP}-\sum_{NSOS}prob\cdot Penalties^N_{SMB}\\[2ex]
+\displaystyle\sum_{NSOS}prob\cdot C^{N'}_{Purchase}
\end{array}
\right)\\[2ex]
-\displaystyle\sum_{NSOS}prob\cdot B^{N'}_{Sell}+\sum_{NSOS}prob\cdot C^{M'}_{DRP}\\[2ex]
-\displaystyle\sum_{NSOS}prob\cdot Penalties^N_{PLOT}
\end{array}
\right)
$$

$\forall X \in CHP, ACH, CCH, PV, WT, PLOT, ESS, CSS, TSS, Boiler, CV$, $Electrical\ Switch$

$\forall Y \in District\ Cooling, District\ Heating, Electrical\ Feeder$

$\forall M \in Electrical\ Load, Heating\ Load, Cooling\ Load\ of\ Smart\ Building$

$\forall N \in Electricity, Heating, and\ Cooling\ Energy\ Carriers\ of\ Smart\ Building$

$\forall N' \in Ancillary\ Services\ of\ Smart\ Building$

$\forall M'' \in Electrical\ Load\ of\ Parking\ Lot$

$\forall N'' \in Active\ Power\ and\ Ancillary\ Services\ of\ Parking\ Lot$

(1)

The objective function is categorized into following groups: 1) the investment costs plus aggregated operating costs of: CHP, absorption chiller, compression chiller, photovoltaic array, wind turbine, parking lot, electrical energy storage, cool storage system, thermal storage system, boiler, district heating and cooling system control valves, and

kVAr

(c)

kVAr

(d)

kW

(e)

kW
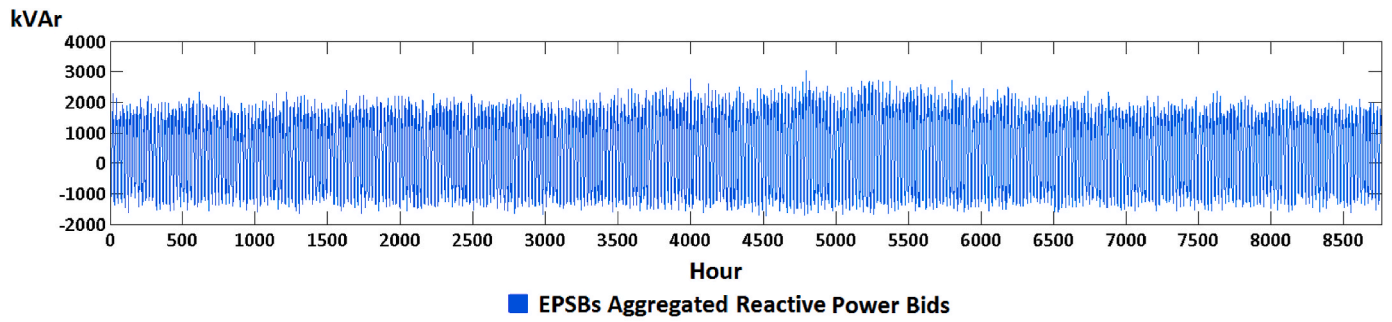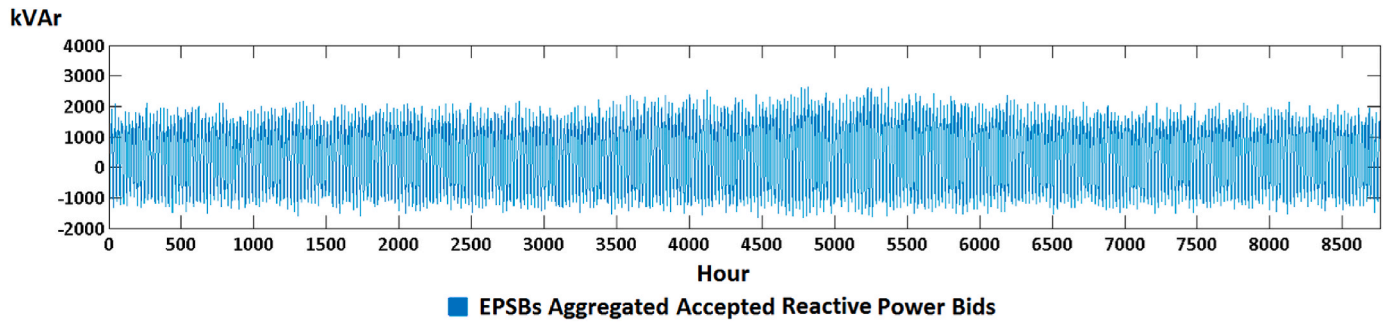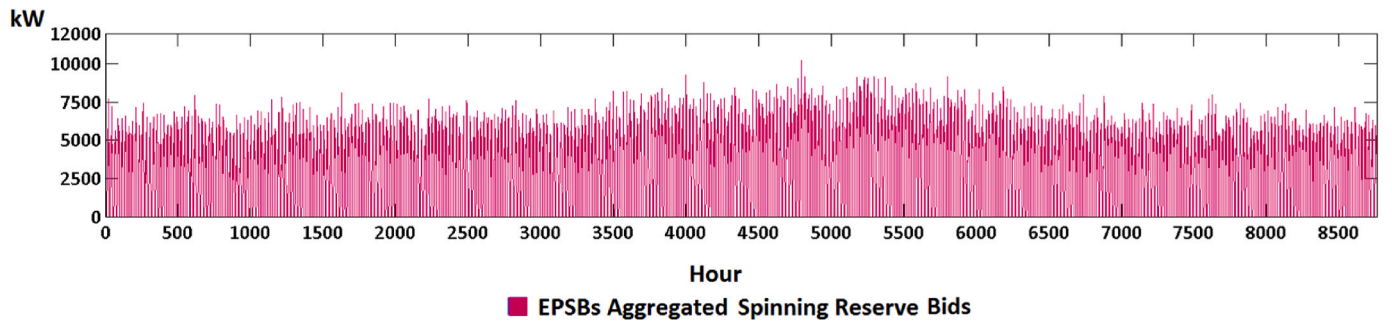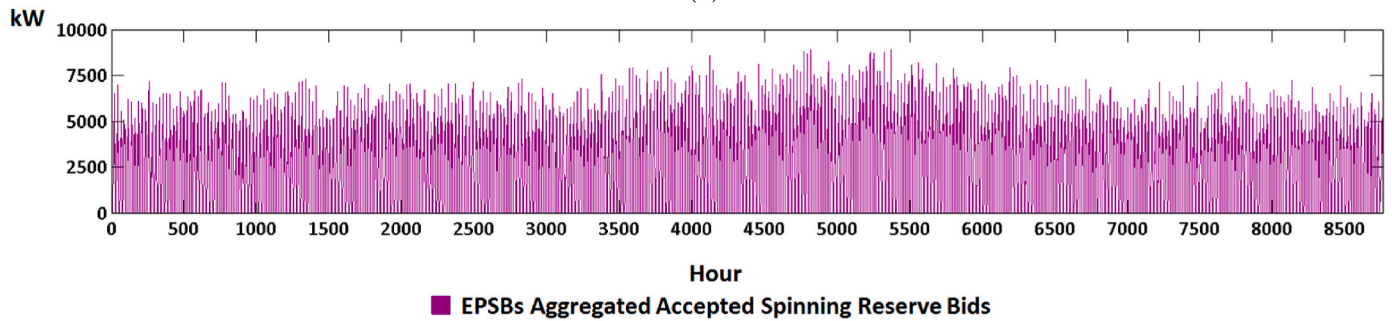
(f)

Fig. 7. (*continued*).

electrical feeder switches $\left(\sum\limits_{XsiteXtype} \sum \psi^X \cdot (C_{Invest}^X + \sum\limits_{Xotime} \tau_X \cdot C_{Op}^X) \right)$; 2) the investment and aggregated operational costs of district heating pipe, district cooling pipe, and electrical feeders $\sum\limits_{YsiteYtype} \sum \psi^Y \cdot \left(C_{Cap}^Y + L_X \cdot C_{Length}^Y \right)$; 3) the aggregated energy not supplied costs of electrical loads, heating loads, and cooling loads ($\sum\limits_{NSC} ENSC^M$); 4) the aggregated costs of

electricity, heating, and cooling energy carriers purchased from smart buildings ($\sum\limits_{NSOS} prob \cdot C_{Purchase}^N$); 5) the aggregated costs of ancillary services purchased from smart buildings ($\sum\limits_{NSOS} prob \cdot C_{Purchase}^N$); 6) the aggregated profits of electricity, heating, and cooling energy carriers sold to smart buildings ($\sum\limits_{NSOS} prob \cdot B_{Sell}^N$); 7) the aggregated costs of demand response programs of electricity, heating, and cooling energy carriers provided by smart buildings ($\sum\limits_{NSOS} prob \cdot C_{DRP}^M$); 8) the aggregated penalties of

12
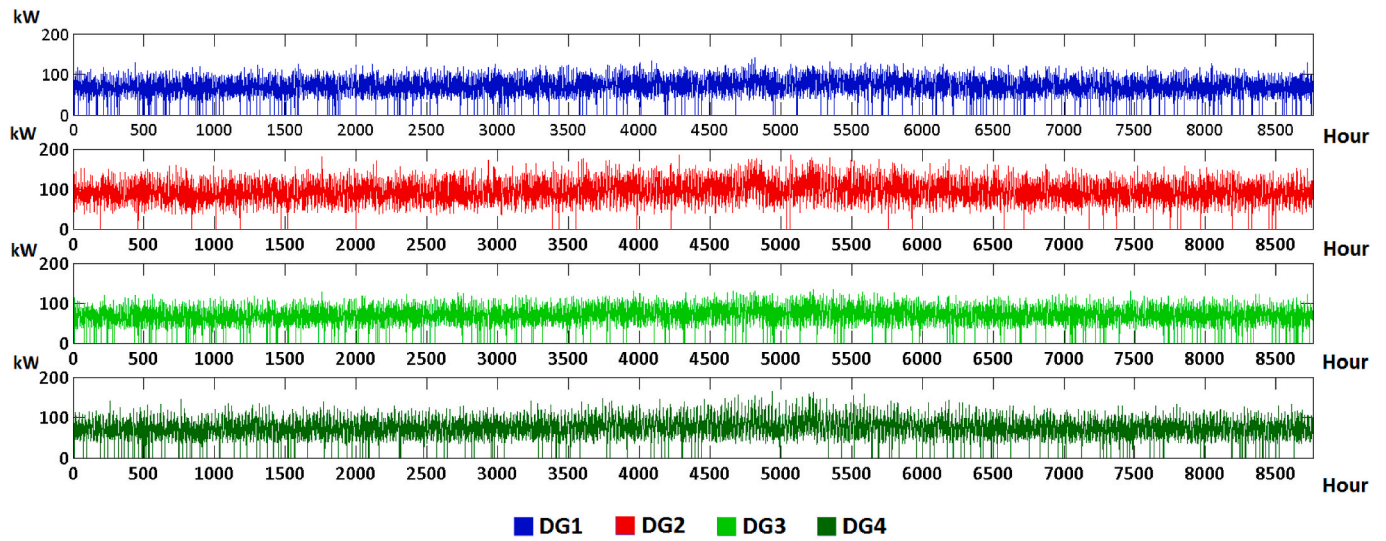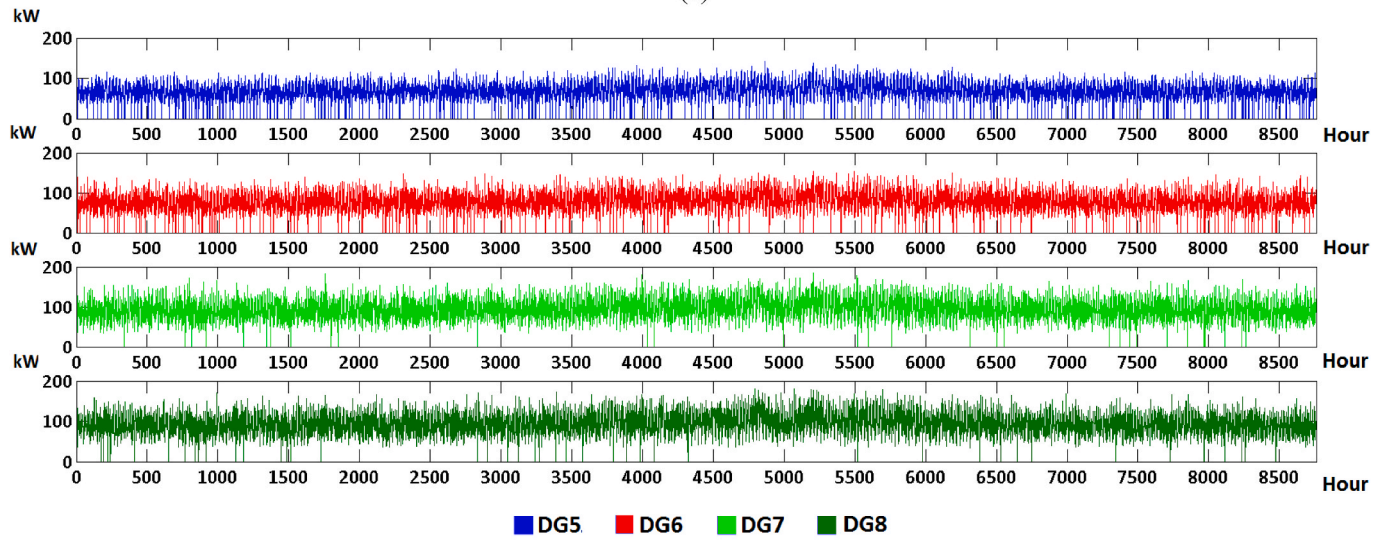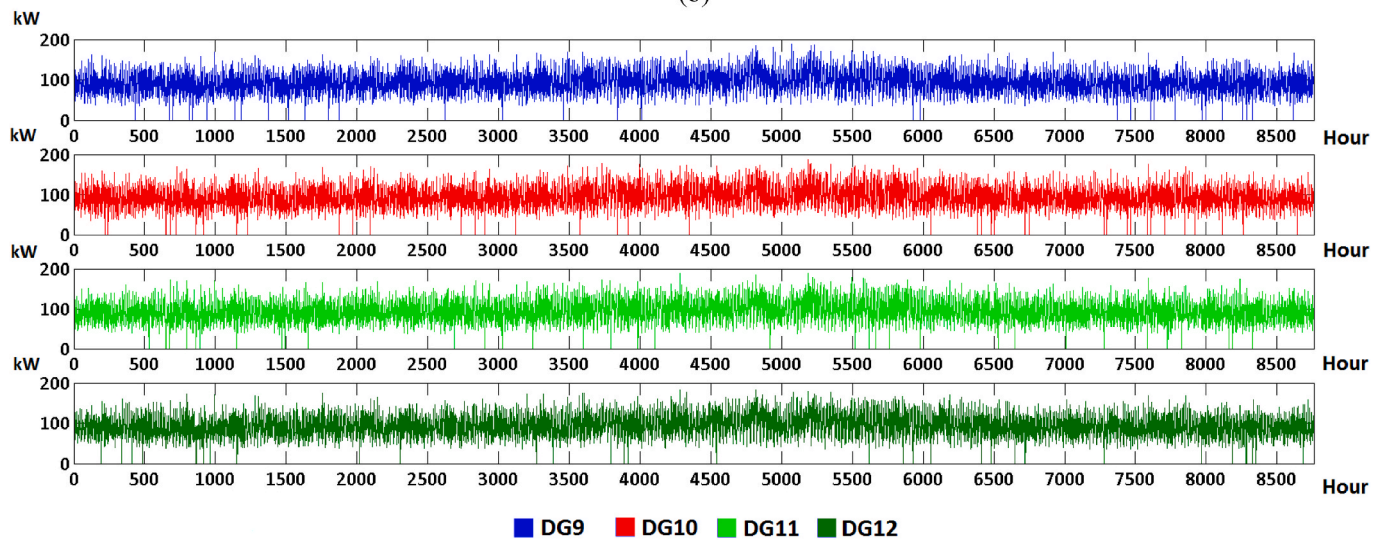
Fig. 8. The estimated values of the active power of 1–4 (a), 5–8 (b), and 9–12 (c) distributed generation for the final year of the planning horizon and the third scenario.
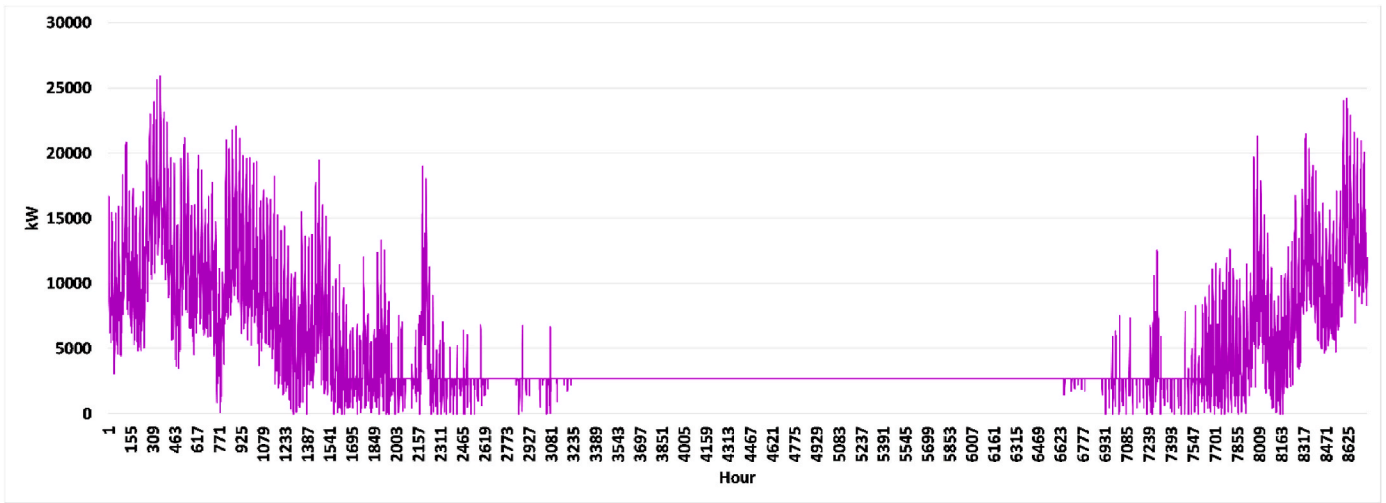
Fig. 9. The estimated values of heating energy generation of boilers for the third scenario and the final planning year.
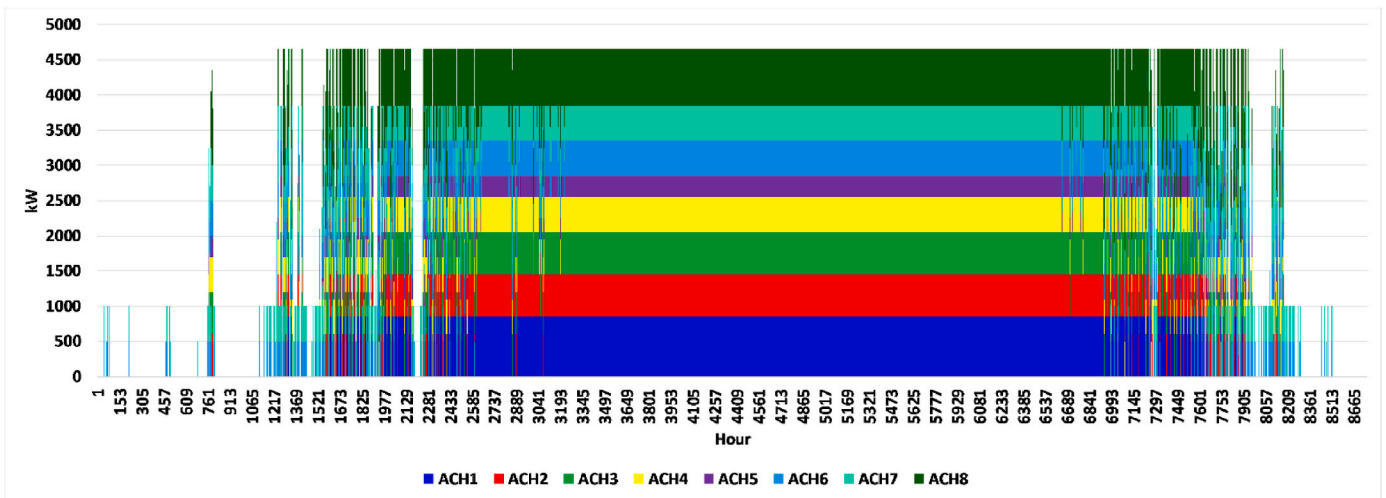
(a)
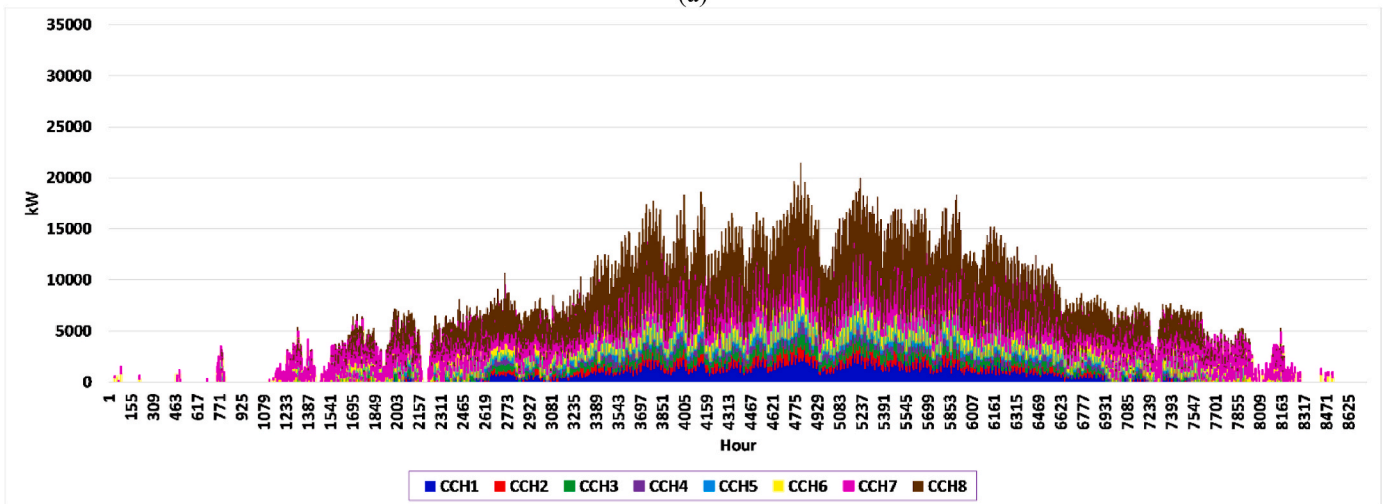
(b)

Fig. 10. (a) The cooling energy generation of absorption chillers for the final year of planning and the third scenario. (b) The cooling energy generation of compression chillers for the final year of planning and the third scenario.

mismatches of electricity and ancillary services, heating, and cooling energy carriers of smart buildings ($\sum_{NSOS} prob \cdot Penalties_{SMB}^{N}$); 9) the

aggregated costs of electricity and ancillary services purchased from parking lots ($\sum_{NSOS} prob \cdot C_{Purchase}^{N}$); 10) the aggregated profits of electricity
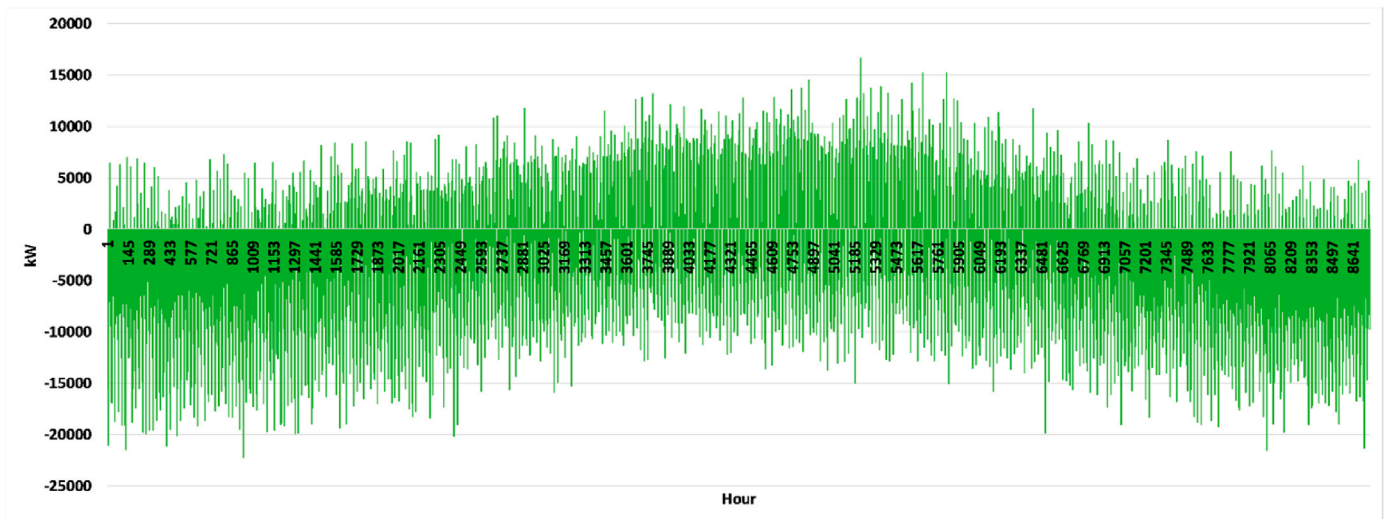
Fig. 11. The electrical energy transactions with the upward electricity market for the final year of planning and the third scenario.

EPSBs Aggregated Active Power Bids

(a)

EPSBs Aggregated Accepted Power Bids

(b)
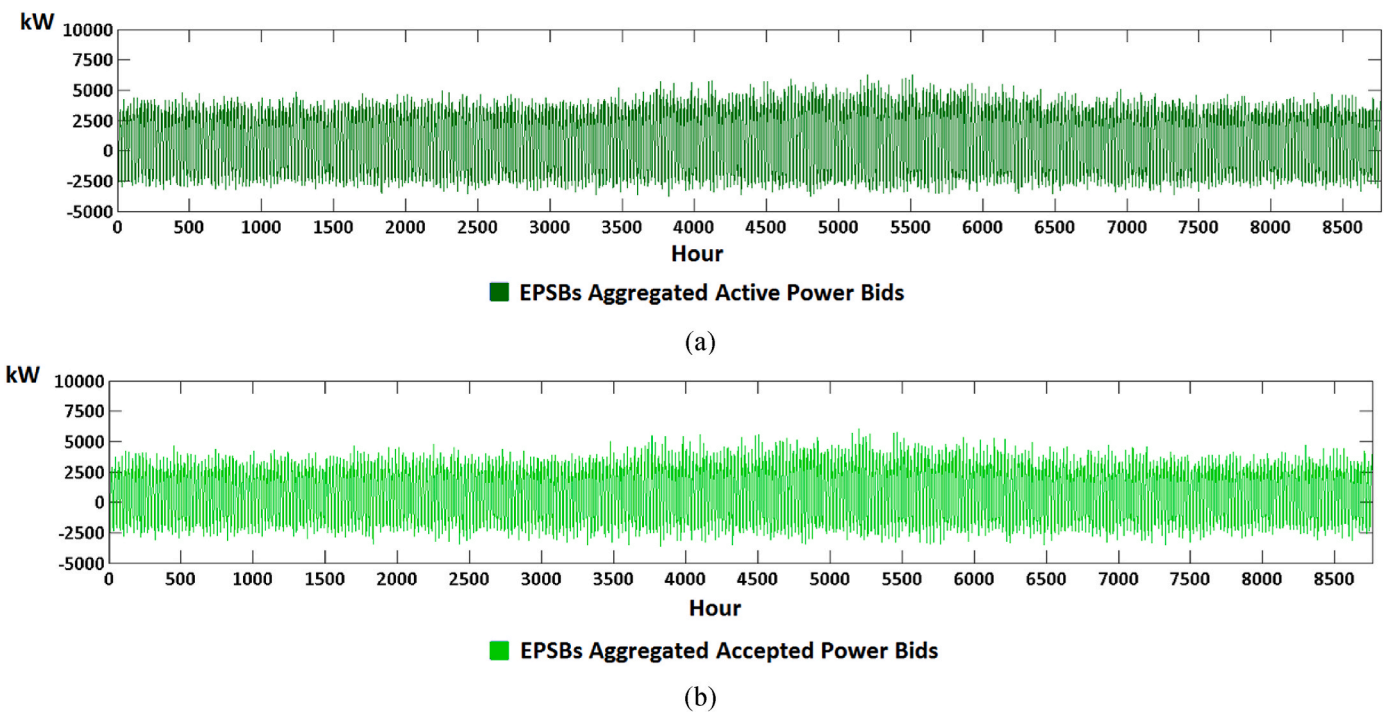
Fig. 12. The submitted values of EPSBs' active power (a), the accepted values of EPSBs' active power (b), the submitted values of EPSBs' reactive power (c), the accepted values of EPSBs' reactive power (d), the submitted values of EPSBs' spinning reserve (e), and the accepted values of EPSBs' spinning reserve (f) of distributed generation for the final year of planning and the fourth scenario.

and ancillary services sold to parking lots ($\sum_{NSOS} prob \cdot B_{Sell}^{N'}$); 11) the aggregated costs of demand response programs of electricity provided by parking lots ($\sum_{NSOS} prob \cdot C_{DRP}^{M'}$); and 12) the aggregated penalties of mismatches of electricity and ancillary services consumption/generation of parking lots ($\sum_{NSOS} prob \cdot Penalties_{PLOT}^{N'}$).

The first stage optimization process constraints are decomposed into 1) energy and mass balance equations; 2) the device loading constraints; 3) minimum and maximum flow constraints of district heating and cooling networks; 4) AC load-flow; 5) the electricity, heating, and cooling demand-supply balancing constraints; 6) radiality constraints of

electrical, district heating, and cooling networks; 7) the static-security constraints of the electrical network; and 8) electricity, heating, and cooling demand response programs constraints [16].

The described constraints are available in Ref. [16] and are not presented for the sake of space.
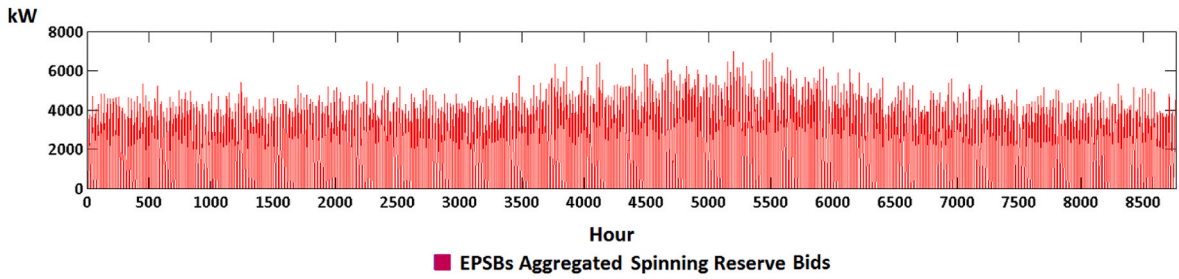
2.4. Second stage problem formulation

The smart building objective function for the second stage problem is the maximization of his/her profits, which can be written as (2):
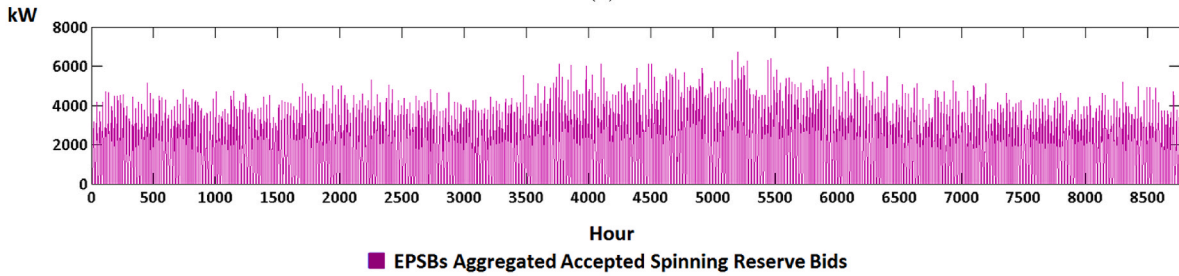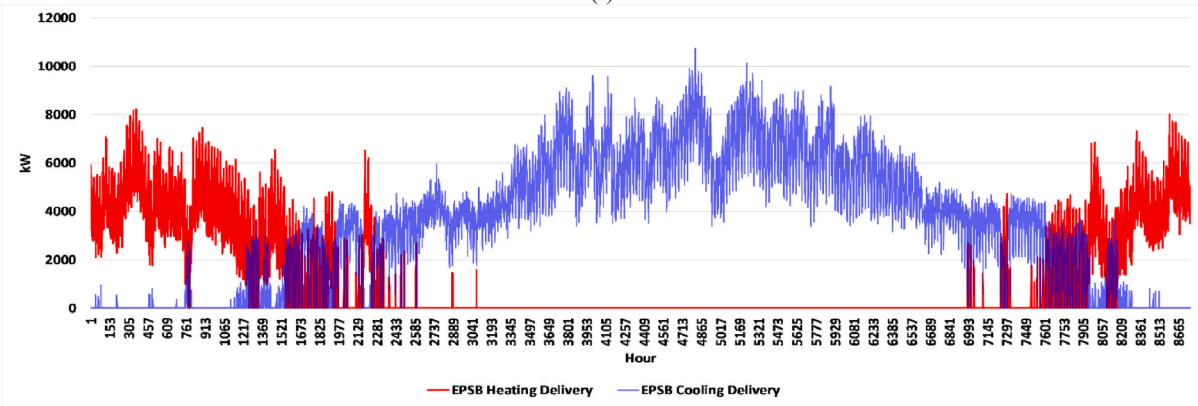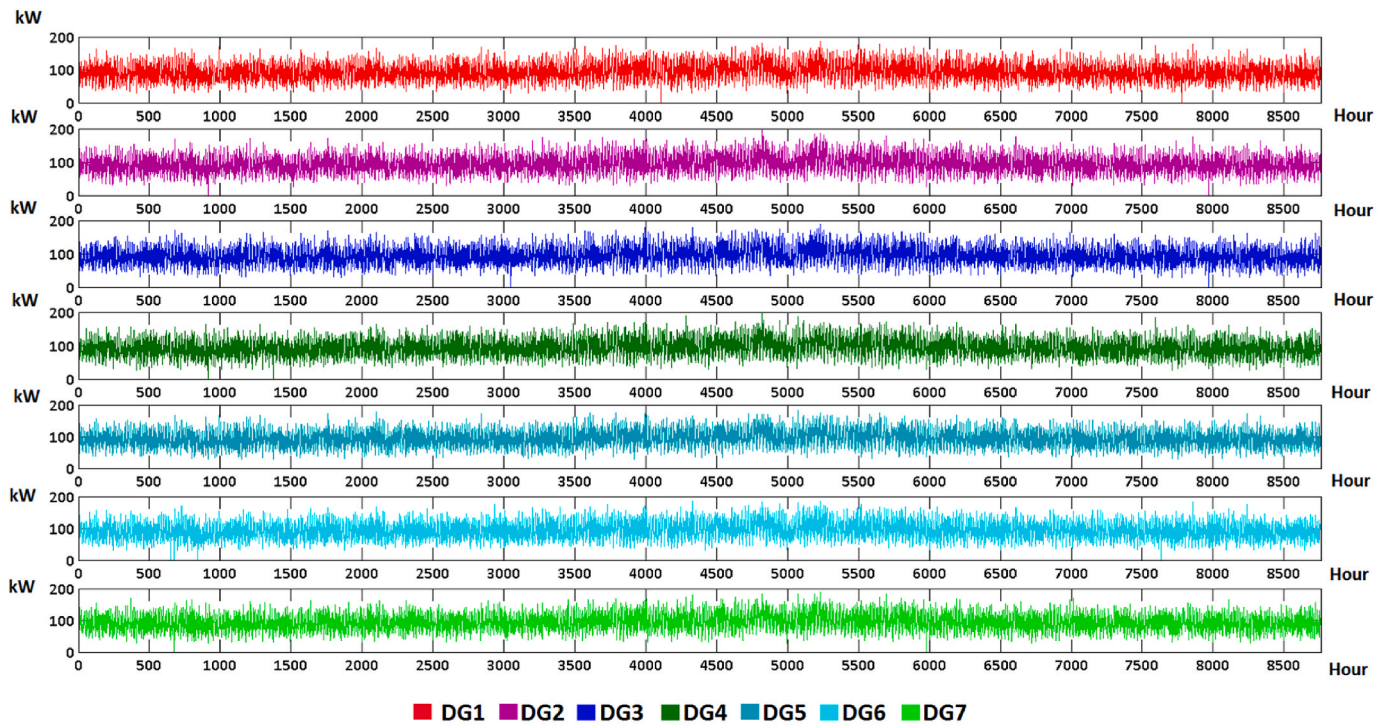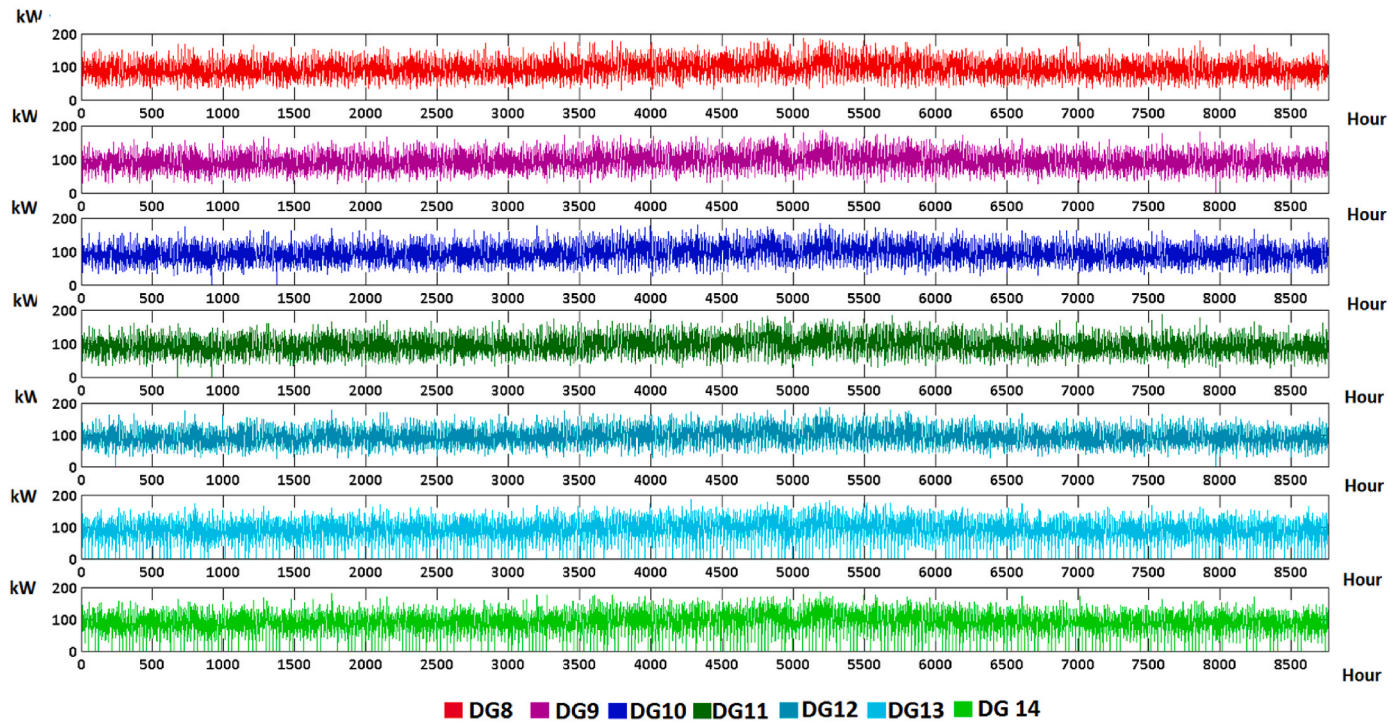
15
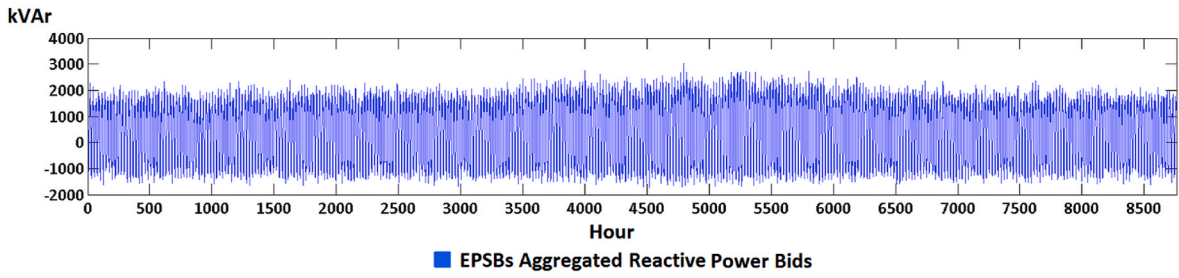
(c)
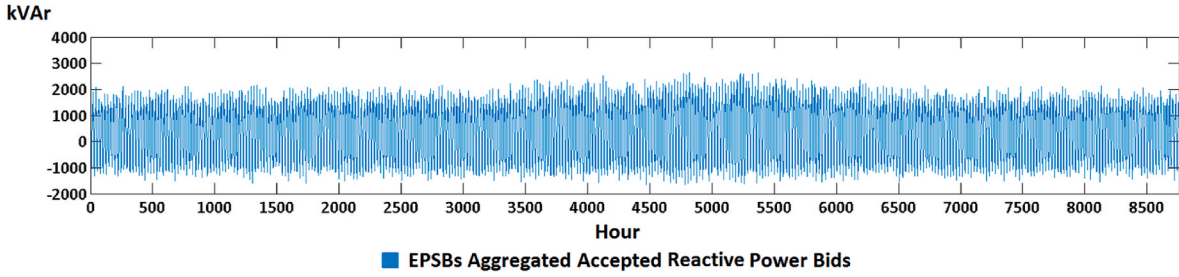
(d)

(e)

(f)

(g)

Fig. 12. (*continued*).

(a)

(b)

Fig. 13. The estimated values of the active power of 1–7 (a), and 8–14 (b) distributed generation for the final year of planning and the fourth scenario.

$$Max\ \mathfrak{A}_{SMB} = \sum_T \sum_{NSMBOS} prob \cdot \begin{pmatrix} -C_{SMB}^{PV} - C_{SMB}^{WT} - C_{SMB}^{CHP} - C_{SMB}^{ACH} - C_{SMB}^{CCH} \\ -C_{SMB}^{Boiler} \\ -C_{SMB}^{ESS} - C_{SMB}^{CSS} - C_{SMB}^{TES} - C_{SMB}^{PHEV} - C_{SMB}^{Purchase} + \\ B_{SMB}^{Sell} + B_{SMB}^{DRP} - \sum Penalty_{SMB} \end{pmatrix}$$

(2)

The objective function is divided into fourteen terms: 1) the operating cost of smart building photovoltaic system (C_{SMB}^{PV}); 2) the operating cost of smart building wind turbine (C_{SMB}^{WT}); 3) the cost of smart building CHP (C_{SMB}^{CHP}); 4) the operating cost of smart building absorption chiller (C_{SMB}^{ACH}); 5) the operating cost of smart building compression chiller (C_{SMB}^{CCH}); 6) the operating cost of smart building boiler (C_{SMB}^{Boiler}); 7) the
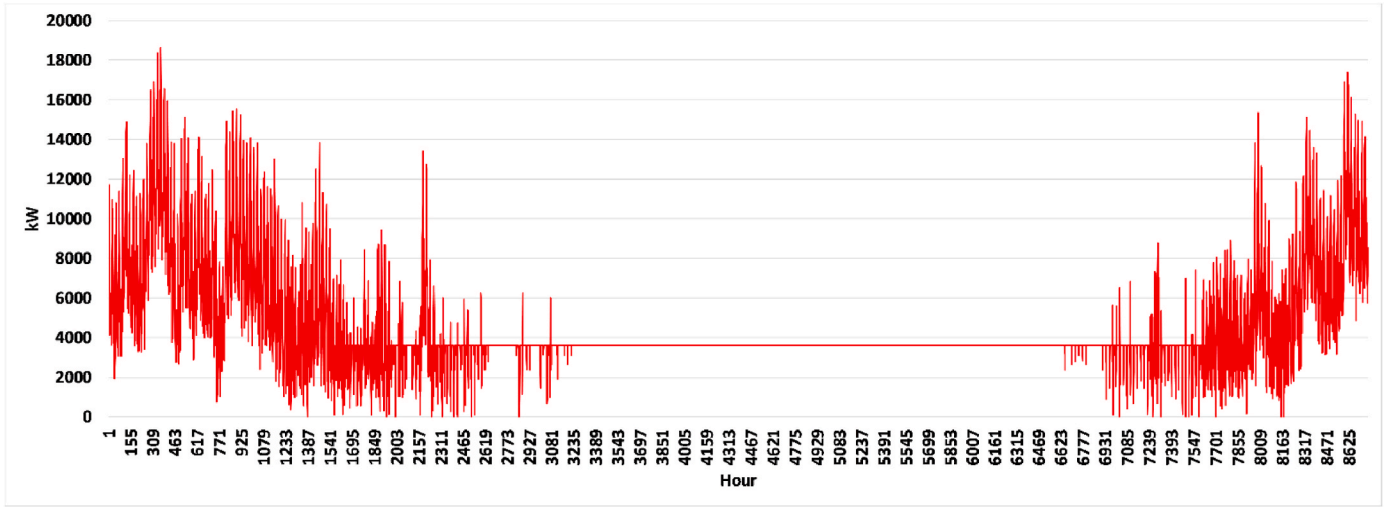
17

Fig. 14. The estimated values of heating energy generation of boilers for the fourth scenario and the final planning year.
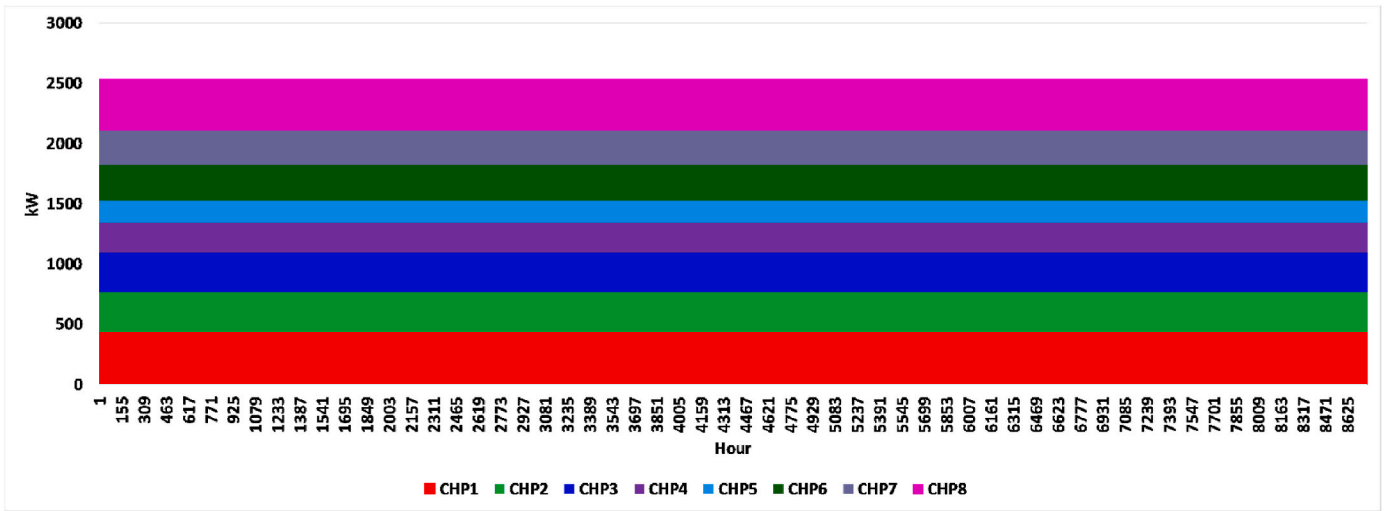

Fig. 15. The electricity generation of combined heat and power generation facilities for the final year of planning and the fourth scenario.

operating cost of smart building electrical storage system (C_{SMB}^{ESS}); 8) the operating cost of smart building cool storage system (C_{SMB}^{CSS}); 9) the operating cost of smart building thermal storage system (C_{SMB}^{TES}); 10) the operating cost of smart building plug-in electric vehicle parking lot (C_{SMB}^{PHEV}); 11) the aggregated costs of electricity, ancillary services, heating, and cooling energy carriers purchased from energy system ($C_{SMB}^{Purchase}$); 12) the aggregated profits of active power, ancillary services, heating, and cooling energy carriers sold to energy system (B_{SMB}^{Sell}); 13) the aggregated profits of demand response programs of electricity, heating, and cooling energy carriers provided by smart building (B_{SMB}^{DRP}); and 14) the aggregated penalties of mismatches of electricity and ancillary services, heating, and cooling energy carriers of smart building.

The smart building profits of active power, ancillary services, heating, and cooling energy carriers sold to the energy system can be written as (3):

$$B_{SMB}^{Sell} = \left(\begin{array}{l} \sum \lambda^{SR} \cdot SR_{SMB} + \sum \lambda^{active} \cdot P_{SMB} + \\ \sum \lambda^{reactive} \cdot Q_{SMB} + \sum \lambda^{Heat} \cdot \varpi_{SMB}^{Heat} + \sum \lambda^{Cool} \cdot \varpi_{SMB}^{Cool} \end{array} \right) \quad (3)$$

Eq. (3) decomposes into the following terms: 1) the profit of smart building spinning reserve sold to the energy system ($\sum \lambda^{SR} \cdot SR_{SMB}$); 2) the profit of smart building active power sold to the energy system

($\sum \lambda^{active} \cdot P_{SMB}$); 3) the profit of smart building reactive power sold to the energy system ($\sum \lambda^{reactive} \cdot Q_{SMB}$); 4) the profit of smart building heating power sold to the energy system ($\sum \lambda^{Heat} \cdot \varpi_{SMB}^{Heat}$); and 5) the profit of smart building cooling power sold to the energy system ($\sum \lambda^{Cool} \cdot \varpi_{SMB}^{Cool}$).

It is assumed that the PHEV parking lots can sell electrical active power, reactive power, and reserve to the energy system. Thus, the PHEV parking lot objective function for the second stage problem is the maximization of PHEV parking lot owner profits that can be written as (4):

$$Max\ \mathfrak{A}_{PLOT} = \sum_{T} \sum_{NPLOTOS} prob \cdot \left(\begin{array}{l} -C_{PLOT}^{PV} - C_{PLOT}^{ESS} - C_{PLOT}^{Purchase} + \\ B_{PLOT}^{Sell} + B_{PLOT}^{DRP} - \sum Penalty_{PLOT} \end{array} \right) \quad (4)$$

The objective function is divided into six terms: 1) the operating cost of the parking lot photovoltaic system (C_{PLOT}^{PV}); 2) the operating cost of the parking lot electrical storage system (C_{PLOT}^{ESS}); 3) the aggregated costs of electricity and ancillary services purchased from the energy system ($C_{PLOT}^{Purchase}$); 4) the aggregated profits of active power and ancillary services sold to the energy system (B_{PLOT}^{Sell}); 5) the aggregated profits of electrical demand response programs provided by the parking lot (B_{PLOT}^{DRP}); and 6) the aggregated penalties of mismatches of electricity and ancillary services of the parking lot.
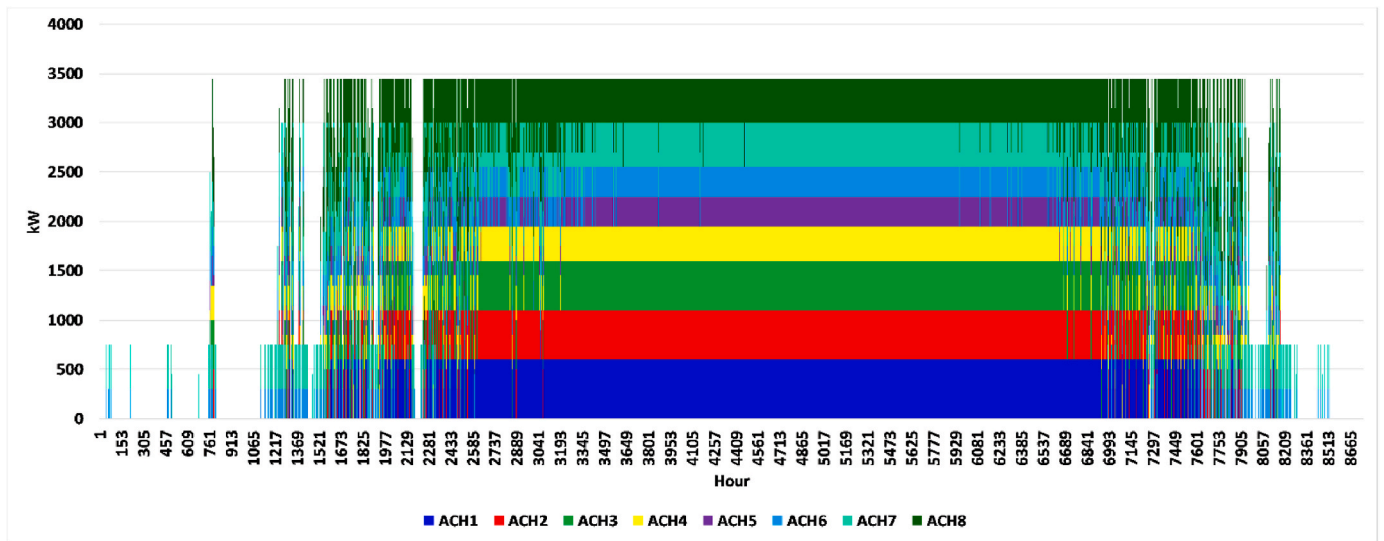
(a)
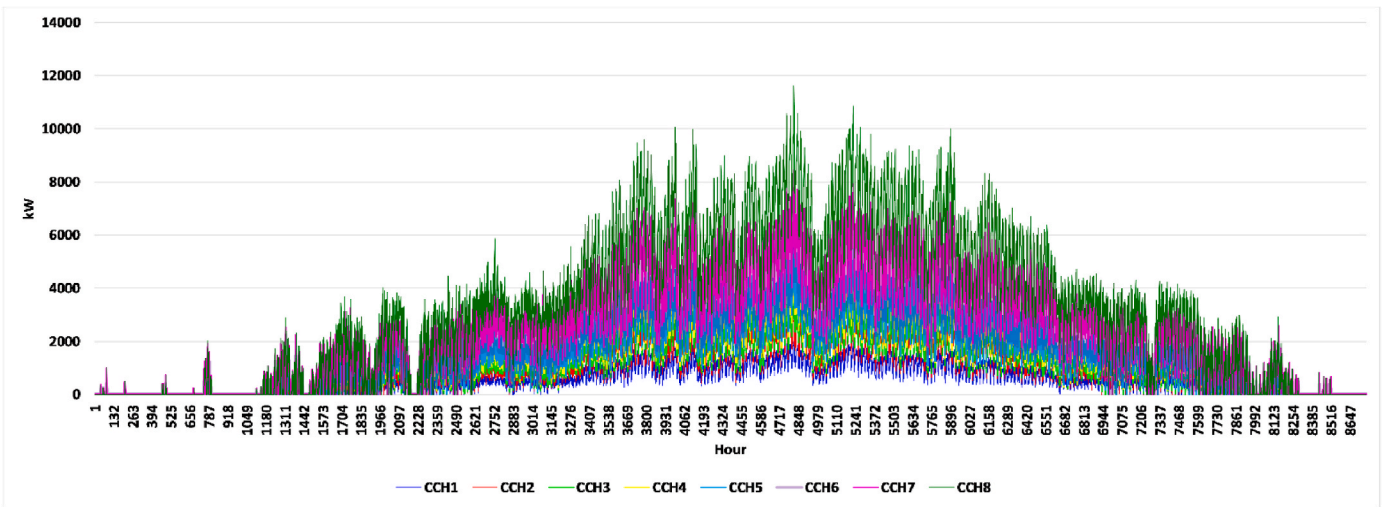
(b)

Fig. 16. (a) The cooling energy generation of absorption chillers for the final year of planning and the fourth scenario. (b) The cooling energy generation of compression chillers for the final year of planning and the fourth scenario.
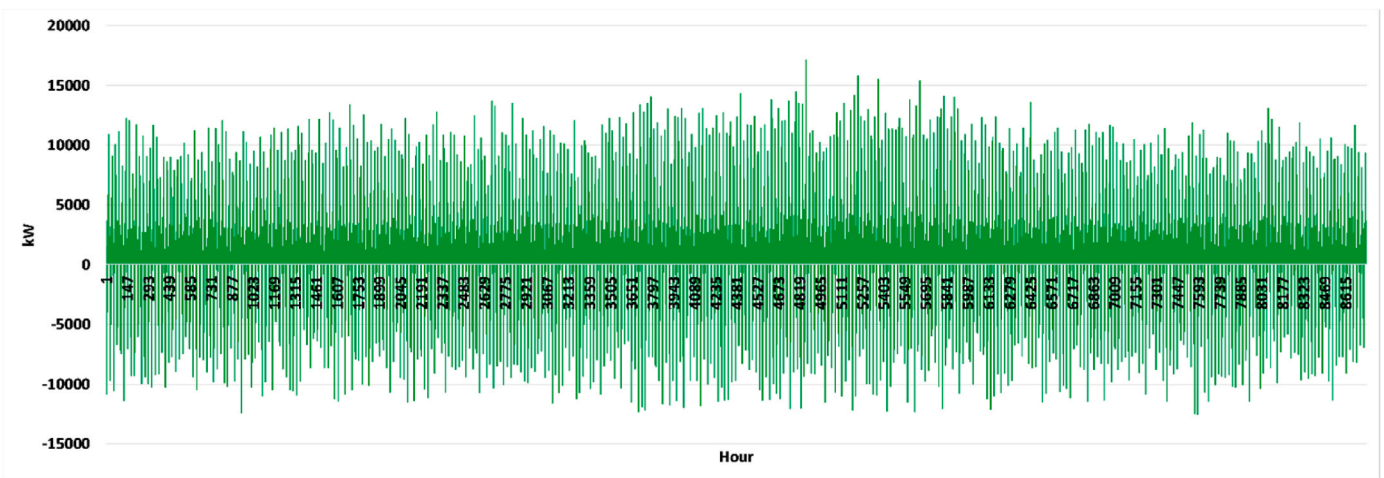

Fig. 17. The electricity transactions of PHEVs with the energy system for the final year of planning and the fourth scenario.

The second stage problem constraints for the PHEV parking lot are decomposed into 1) electrical energy balance equations for each parking lot internal system; 2) the device loading constraints; and 3) the electrical demand response programs constraints [16]. The PHEV model and

constraints are available in Ref. [28] and are not presented for the sake of space.

2.5. Third stage problem formulation

The energy system should minimize the energy procurement and energy interruption costs for the hourly operational scheduling process. The objective function of the third stage problem is the minimization of system costs, which can be written as (5):

$$Min\ \mathbb{Z} = \sum_T \sum_{NSOS} prob. \begin{pmatrix} W_1 \cdot \backslash\backslash (C_{ES}^{PV} + C_{ES}^{WT} + C_{ES}^{ACH} + C_{ES}^{CCH} + C_{ES}^{CHP} \\ +C_{ES}^{ESS} + \\ C_{ES}^{Boiler} + C_{ES}^{CSS} + C_{ES}^{TES} + C_{Purchase}^{N} + C_{Purchase}^{N'} \\ +C_{DRP}^{M} - B_{Sell}^{N} - \\ Penalties_{SMB}^{N} + C_{Purchase}^{N'} - B_{Sell}^{N'} + C_{DRP}^{M'} \\ -Penalties_{PLOT}^{N'} \\ +W_2 \cdot \sum_{NSC} prob. \mathbb{k}_{CS} \end{pmatrix} \tag{5}$$

$\forall M \in Electrical\ Load, Heating\ Load, Cooling\ Load\ of\ Smart\ Building$

$\forall N \in Electricity, Heat, and\ Cool\ Energy\ Carriers\ of\ Smart\ Building$

$\forall N' \in Ancillary\ Services\ of\ Smart\ Building$

$\forall M'' \in Electrical\ Load\ of\ Parking\ Lot$

$\forall N'' \in Active\ Power\ and\ Ancillary\ Services\ of\ Parking\ Lot$

The objective function is divided into nineteen terms: 1) the operating cost of energy system photovoltaic system (C_{ES}^{PV}); 2) the operating cost of energy system wind turbine (C_{ES}^{WT}); 3) the operating cost of energy system absorption chiller (C_{ES}^{ACH}); 4) the operating cost of energy system compression chiller (C_{ES}^{CCH}); 5) the cost of energy system CHP (C_{ES}^{CHP}); 6) the operating cost of energy system electrical storage system (C_{ES}^{ESS}); 7) the operating cost of energy system boiler (C_{ES}^{Boiler}); 8) the operating cost

of energy system cool storage system (C_{ES}^{CSS}); 9) the operating cost of energy system thermal storage system (C_{SMB}^{TES}); 10) the aggregated costs of electricity, heating, and cooling energy carriers purchased from smart buildings ($C_{Purchase}^{N}$); 11) the aggregated costs of ancillary services purchased from smart buildings ($C_{Purchase}^{N'}$); 12) the aggregated costs of demand response programs of electricity, heating, and cooling energy carriers provided by smart buildings (C_{DRP}^{M}); 13) the aggregated profits of electricity, heating, and cooling energy carriers sold to smart buildings (B_{Sell}^{N}); 14) the aggregated penalties of mismatches of electricity and ancillary services, heating, and cooling energy carriers of smart buildings ($Penalties_{SMB}^{N}$); 15) the aggregated costs of electricity and ancillary services purchased from parking lots ($C_{Purchase}^{N'}$); 16) the aggregated profits of electricity and ancillary services sold to parking lots ($B_{Sell}^{N'}$); 17) the aggregated costs of demand response programs of electricity provided by parking lots ($C_{DRP}^{M'}$); 18) the aggregated penalties of mismatches of electricity and ancillary services consumption/generation of parking lots ($Penalties_{PLOT}^{N'}$); and 19) the weighted expected value of energy system costs in external shock conditions ($W_2 \cdot \sum_{NSCS} prob. \mathbb{k}_{CS}$).

Eq. (5) constraints consist of the following terms: 1) energy and mass balance equations; 2) the device loading constraints; 3) minimum and maximum flow constraints of district heating and cooling networks; 4) AC load-flow; 5) the electricity, heating, and cooling demand-supply balancing constraints; 6) the static-security constraints of the electrical network; and 7) electricity, heating, and cooling demand response programs constraints [16]. Further, the parking lots' charge and discharge constraints, their minimum and maximum limits of charge constraints, and the maximum charge limits are also considered in the optimization procedure and are not presented for the sake of space [28].

A Self-healing Performance Index (SPI) is proposed to assess the level of self-healing of the multi-carrier energy system in the worst-case conditions. The SPI is defined as (6):

$$SPI = \frac{\sum Served\ Electrical\ Loads\ in\ Contingent\ Conditions}{\sum Served\ Electrical\ Loads\ in\ Normal\ Conditions - \sum Served\ Electrical\ Loads\ in\ Contingent\ Conditions} \\ + \frac{\sum Served\ Heating\ Loads\ in\ Contingent\ Conditions}{\sum Served\ Heating\ Loads\ in\ Normal\ Conditions - \sum Served\ Heating\ Loads\ in\ Contingent\ Conditions} \\ + \frac{\sum Served\ Cooling\ Loads\ in\ Contingent\ Conditions}{\sum Served\ Cooling\ Loads\ in\ Normal\ Conditions - \sum Served\ Cooling\ Loads\ in\ Contingent\ Conditions} \tag{6}$$
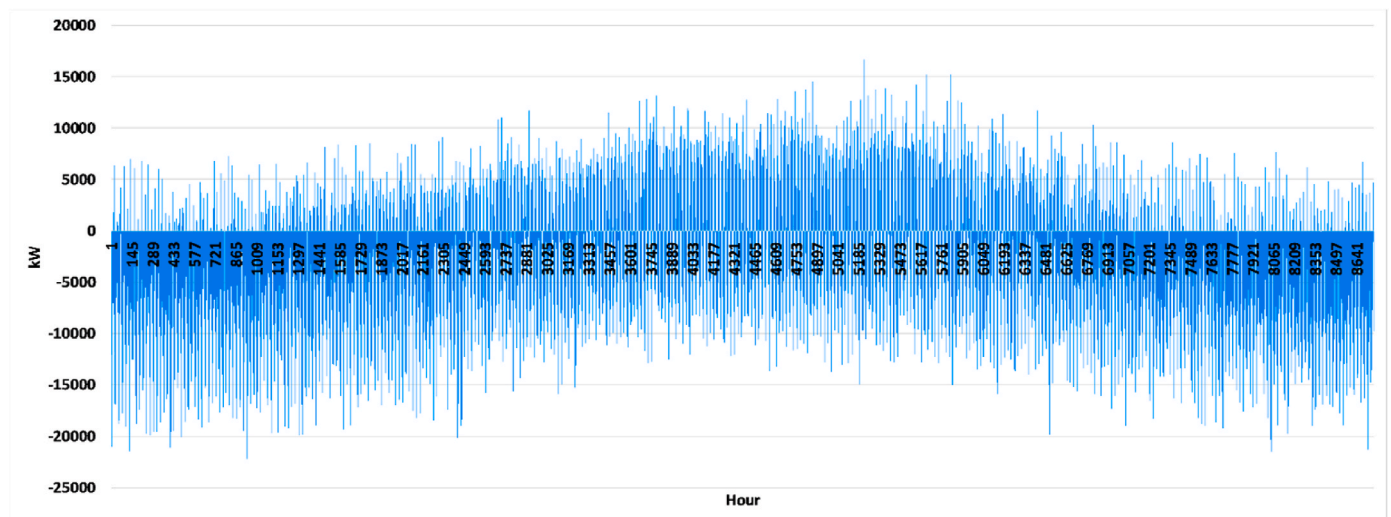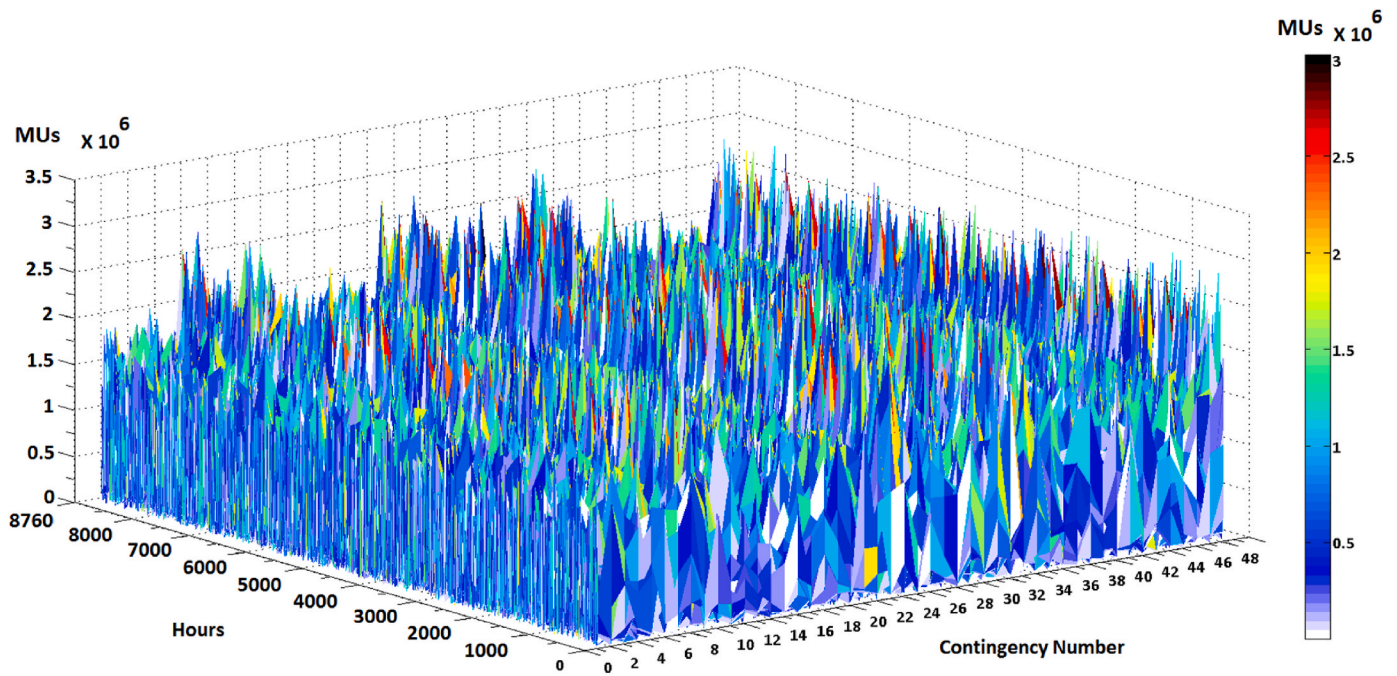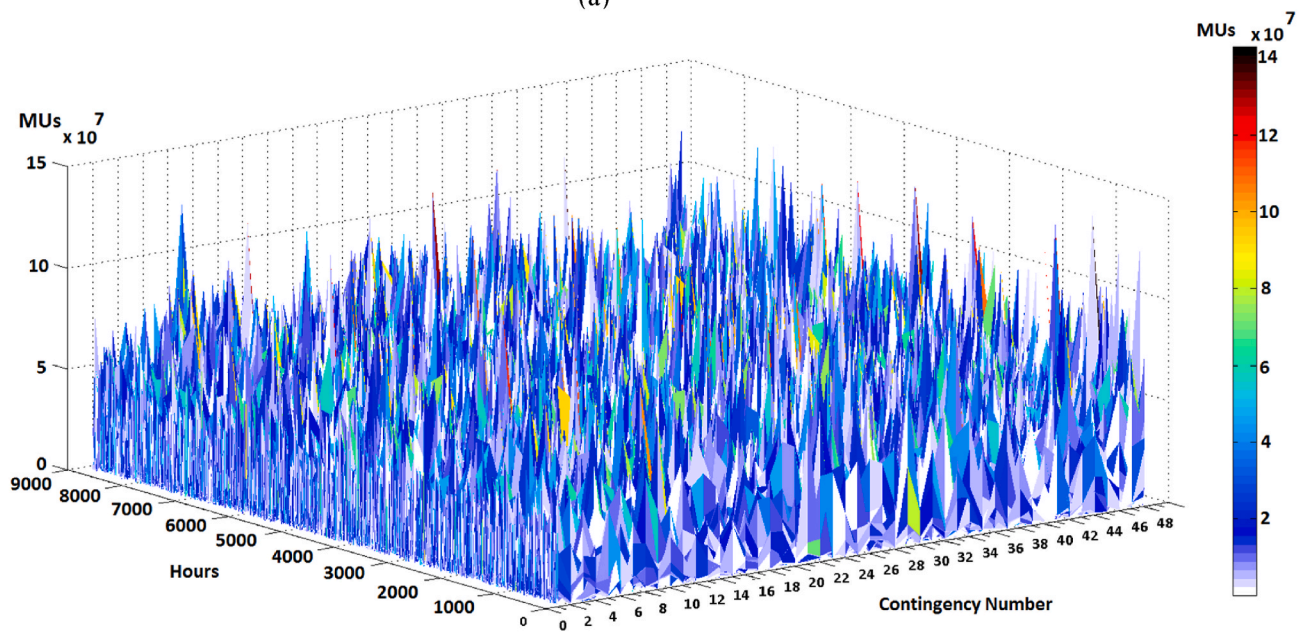

Fig. 18. The electrical energy transactions with the upward electricity market for the final year of planning and the fourth scenario.

(a)

(b)

Fig. 19. The aggregated operational and interruption costs of the system for the 48 worst-case external shocks for the fourth (a) and the first scenario (b).

2.6. Fourth stage problem formulation

The fourth stage optimization process optimizes the topology of the system and the scheduling of resources in external shock conditions. It is assumed that the external shock segments the energy system into secured and on-outage zones. The energy system zones that are not affected by the external shock should be optimally dispatched by the third stage optimization process. The critical electrical, heating, and cooling loads of on-outage zones should be restored using the fourth stage optimization process. The objective function for the shock-affected zones can be formulated as (7):
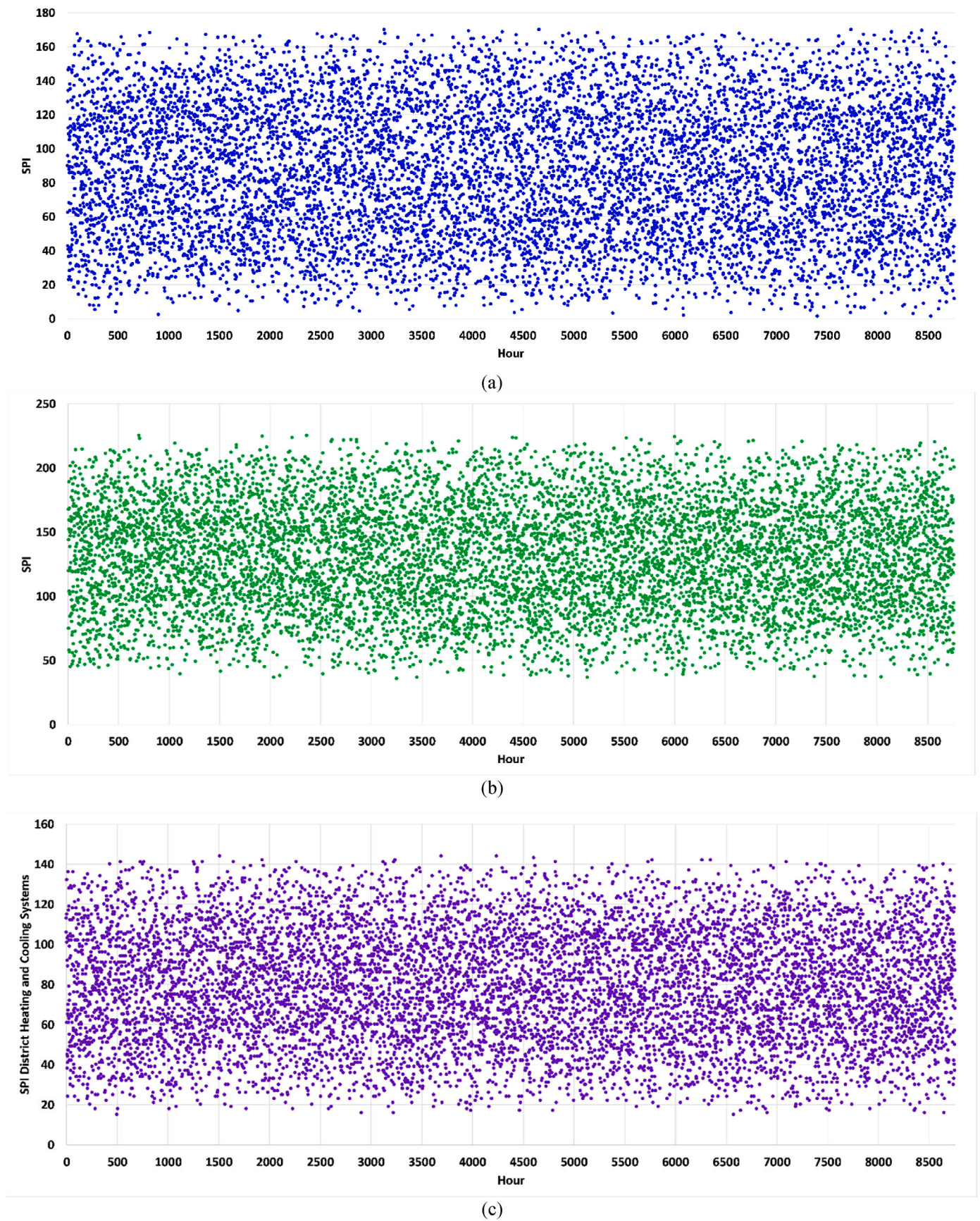
(a)

(b)

(c)

Fig. 20. (a) The self-healing performance index for the designed system of the first scenario and 48 worst-case external shocks. (b) The SPI for the designed system of the second scenario. (c) The SPI for the district heating and cooling designed systems of the third scenario.
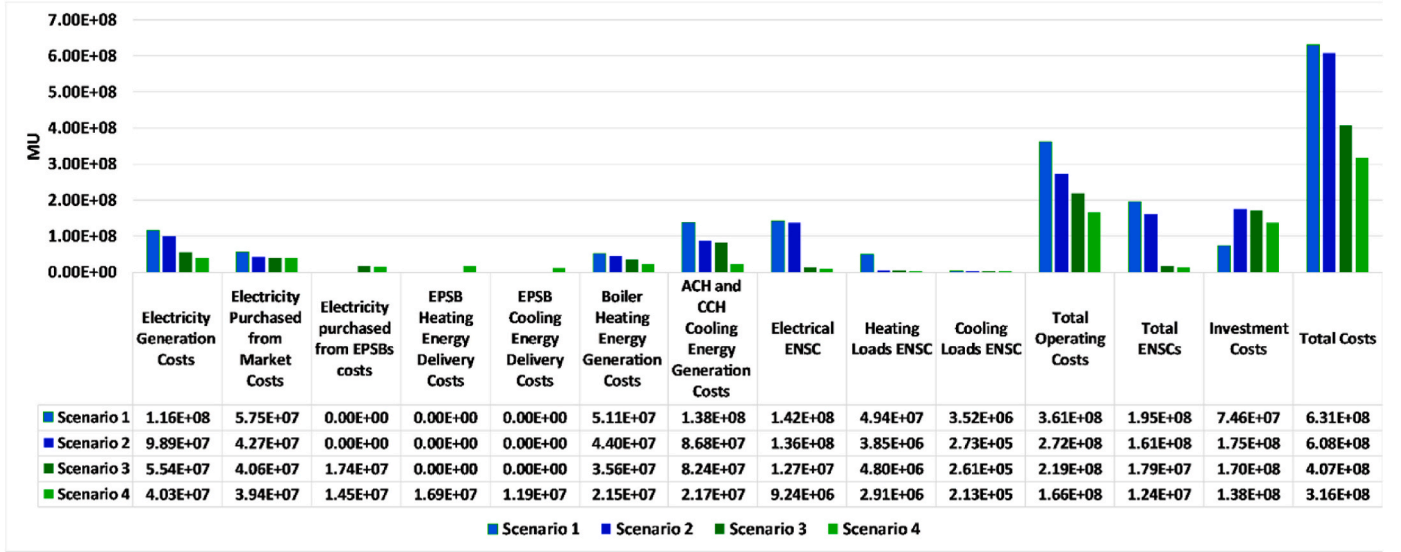
	Electricity Generation Costs	Electricity Purchased from Market Costs	Electricity purchased from EPSBs costs	EPSB Heating Energy Delivery Costs	EPSB Cooling Energy Delivery Costs	Boiler Heating Energy Generation Costs	ACH and CCH Cooling Energy Generation Costs	Electrical ENSC	Heating Loads ENSC	Cooling Loads ENSC	Total Operating Costs	Total ENSCs	Investment Costs	Total Costs
Scenario 1	1.16E+08	5.75E+07	0.00E+00	0.00E+00	0.00E+00	5.11E+07	1.38E+08	1.42E+08	4.94E+07	3.52E+06	3.61E+08	1.95E+08	7.46E+07	6.31E+08
Scenario 2	9.89E+07	4.27E+07	0.00E+00	0.00E+00	0.00E+00	4.40E+07	8.68E+07	1.36E+08	3.85E+06	2.73E+05	2.72E+08	1.61E+08	1.75E+08	6.08E+08
Scenario 3	5.54E+07	4.06E+07	1.74E+07	0.00E+00	0.00E+00	3.56E+07	8.24E+07	1.27E+07	4.80E+06	2.61E+05	2.19E+08	1.79E+07	1.70E+08	4.07E+08
Scenario 4	4.03E+07	3.94E+07	1.45E+07	1.69E+07	1.19E+07	2.15E+07	2.17E+07	9.24E+06	2.91E+06	2.13E+05	1.66E+08	1.24E+07	1.38E+08	3.16E+08

Fig. 21. The final investment costs, energy not supplied costs, electricity generation costs, and operating costs for considered scenarios at the horizon year of planning.

$$
\begin{aligned}
Min\ \mathbb{k}_{CS} = W_3 \cdot \Bigg[&\sum_{NESAzone} \begin{pmatrix} C^{PV}_{Available\ ES} + C^{WT}_{Available\ ES} + C^{ACH}_{Available\ ES} + C^{CCH}_{Available\ ES} + C^{CHP}_{Available\ ES} \\ + C^{ESS}_{Available\ ES} + C^{Boiler}_{Available\ ES} + C^{CSS}_{Available\ ES} + C^{TES}_{Available\ ES} + C^{N}_{Available\ Purchase} \\ + C^{N'}_{Available\ Purchase} + C^{M}_{Available\ DRP} - B^{N}_{Available\ Sell} - Penalties^{N}_{Available\ SMB} \\ + C^{N'}_{Available\ Purchase} - B^{N'}_{Available\ Sell} + C^{M'}_{Available\ DRP} - Penalties^{N'}_{Available\ PLOT} \end{pmatrix} \\
&+ \sum_{NSUPPzones} \varphi^{Elctrical\ Switch} \cdot \begin{pmatrix} \Delta C^{CHP}_{SUPPZ\ ES} + \Delta C^{ESS}_{SUPPZ\ ES} + \Delta C^{N}_{SUPPZ\ Purchase} + \Delta C^{N'}_{SUPPZ\ Purchase} + \Delta C^{M}_{SUPPZ\ DRP} \\ - \Delta B^{N}_{SUPPZ\ Sell} + \Delta C^{N'}_{SUPPZ\ Purchase} - \Delta B^{N'}_{SUPPZ\ Sell} + \Delta C^{M'}_{SUPPZ\ DRP} \end{pmatrix}
\end{aligned}
\tag{7}
$$

$$
+ \sum_{NSUPPzones} \varphi^{District\ Heating\ Valve} \cdot \begin{pmatrix} \Delta C^{CHP}_{SUPPZ\ ES} + \Delta C^{N}_{SUPPZ\ Purchase} + \Delta C^{M}_{SUPPZ\ DRP} - \Delta B^{N}_{SUPPZ\ Sell} \\ + \Delta C^{Boiler}_{SUPPZ\ ES} + \Delta C^{TES}_{SUPPZ\ ES} \end{pmatrix} + \sum_{NSUPPzones} \varphi^{District\ Cooling\ Valve} \cdot \begin{pmatrix} \Delta C^{CHP}_{SUPPZ\ ES} + \Delta C^{N}_{SUPPZ\ Purchase} \\ + \Delta C^{M}_{SUPPZ\ DRP} - \Delta B^{N}_{SUPPZ\ Sell} \\ + \Delta C^{Boiler}_{SUPPZ\ ES} + \Delta C^{CSS}_{SUPPZ\ ES} \end{pmatrix} \Bigg]
$$

$$
+ W_4 \cdot \Bigg[\sum_{NESAzone} \left(\sum_{CEL} P^{Load}_{Critical\ ES} \cdot IC_{Electrical\ ES} + \sum_{CHL} H^{Load}_{Critical\ ES} \cdot IC_{Heating\ ES} + \sum_{CCL} R^{Load}_{Critical\ ES} \cdot IC_{Cooling\ ES} \right) \Bigg]
$$

Eq. (7) is decomposed into five following groups.

1) The first group of objective functions is the available energy system distributed energy resources of on-outage zones and the optimization process minimizes the operating costs of the available energy resources.

2) The second group of objective functions minimizes the change of the current operating point of electrical distributed energy resources of secured zones that are supplying the electrical loads of on-outage zones.

3) The third and fourth groups of objectives functions are minimizing the change of the current operating point of heating and cooling distributed energy resources of secured zones, respectively. It is assumed that the energy resources of secured zones are supplying the heating and cooling loads of on-outage zones using ON/OFF control of district heating and cooling control valves.

4) The fifth group of objective functions is the interruption costs of the electrical, heating, and cooling loads. The optimization process minimizes the aggregated interruption costs of on-outage electrical, heating, and cooling loads.

3. Optimization algorithm

The following assumptions are considered in the optimization algorithm.

- The uncertainty of the following parameters is modeled in the optimization process using scenario generation/reduction of autoregressive integrated moving average model: energy partner mode smart buildings biddings, electricity and ancillary services' prices, electrical load profiles, intermittent power generations, parking lots charge, and discharges, and demand response contribution scenarios of saver and comfort modes of smart buildings [29,30].

- Further, the Monte-Carlo stochastic process is utilized to estimate the intensity and location of external shocks [4,30]. The following contingencies are considered as the worst-case external shocks: 1) Triple energy carrier distribution network/pipeline outages and single DER outage; 2) Triple DER outages; and 3) Combination of described outages.

- In the contingent conditions, the model is considered that all of the PHEVs have arrived at parking lots, which are discharged to supply the system loads.
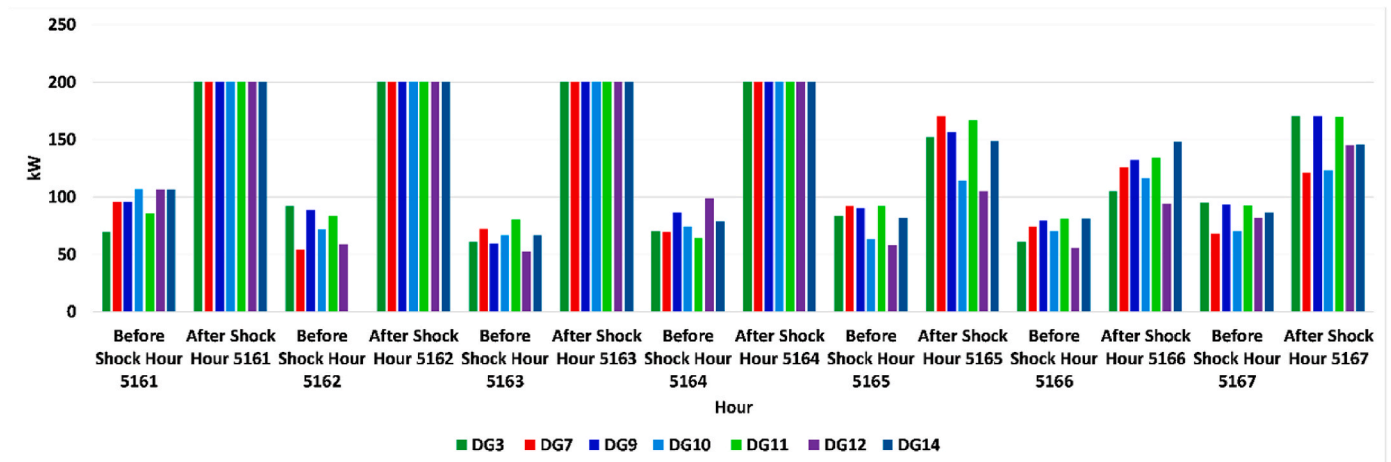
(a)
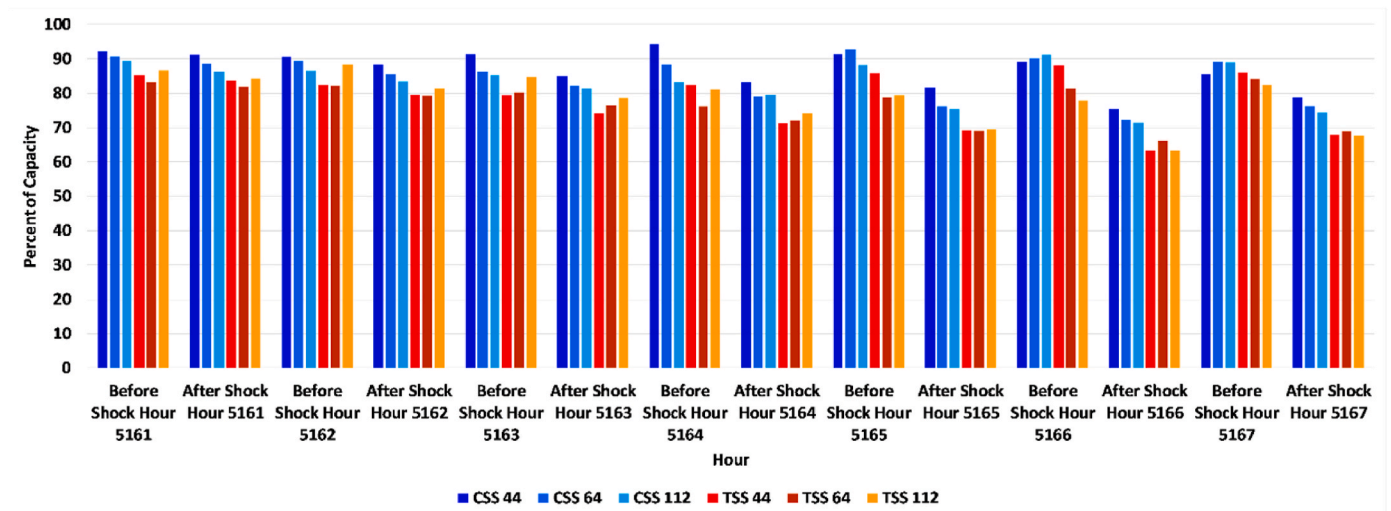
(b)

Fig. 22. (a) The estimated optimal dispatch values of DGs before and after external shock, (b) The estimated optimal dispatch values of CSSs and TSSs before and after external shock, (c) The estimated optimal dispatch values of ESSs before and after external shock, (d) The estimated optimal dispatch values of PHEV parking lots before and after external shock.

- The weighted sum method is utilized to recast the third and fourth-stage problems as multi-objective optimization programs. The detailed process of the method is presented in Ref. [31].

The trade-off between computational complexity and accuracy was a major challenge in this research. The authors had many attempts to propose a framework to solve the very complex OSESP problem. The results of different frameworks and solvers were compared, and finally, the proposed framework was selected.

The proposed four-stage optimization models are mixed integer non-linear programming problems and the formulated problems are solved by the DICOPT solver of GAMS. Fig. 1 depicts the flowchart of the proposed algorithm.

As shown in Fig. 1, the proposed optimization algorithm is an iterative process that is decomposed into optimal planning, optimal bidding strategies of smart buildings and PHEV parking lots, the optimal operational scheduling of system resources in normal conditions, and optimization of system's topology and scheduling of resources in external shock conditions, in the first, second, third, and fourth stages, respectively.

4. Simulation results

The proposed method was assessed by the 123-bus IEEE test system. Fig. 2 presents the modified topology of the 123-bus test system. The scenario generation and reduction scenarios are presented in Table 2.

Tables 3 and 4 present the characteristics of distributed generation and CHP units, respectively. The lifetime of DGs and CHPs is 25 years [16,32]. MUs and MMUs stand for monetary units and million monetary units, respectively. Table 5 shows the characteristics of boilers. The lifetime and maintenance costs of boilers are 25 years and 4.95E+05 (MUs), respectively [32]. Tables 6 and 7 present the input data of the simulation process and load interruption costs, respectively. The wind turbines' lifetime and operating data, photovoltaic systems' lifetime and costs, and chillers data are available in Ref. [33], Ref. [34], and Ref. [35], respectively.

Fig. 3 depicts the estimated values of electrical, heating, and cooling load profiles for the horizon year (2028).

Figs. 4 and 5 depict the forecasted electricity generation of photovoltaic arrays and wind turbines for the final year of the planning horizon,
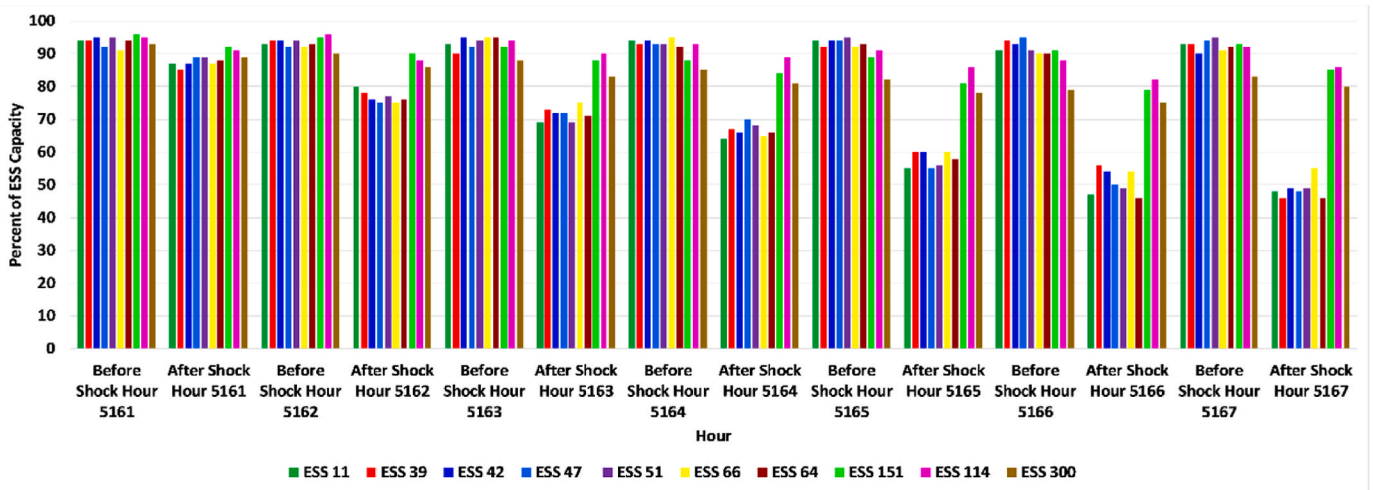
(c)
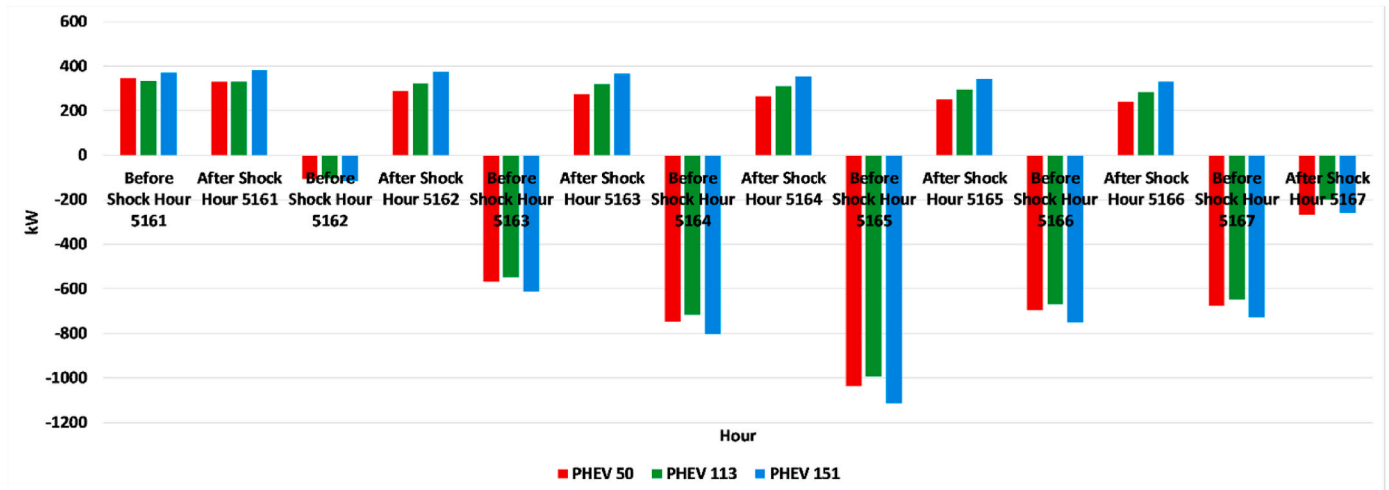
(d)

Fig. 22. (*continued*).

respectively.

Four scenarios were studied to assess the proposed framework.

Scenario 1. The energy system purchased electricity from the utility grid to supply its loads. Only boilers and compression chillers were used to supply the heating and cooling loads.

Scenario 2. The first scenario was implemented and the CCHPs were utilized to supply the heating and cooling loads through district heating and cooling networks.

Scenario 3. The second scenario was implemented considering transaction electricity with the smart buildings.

Scenario 4. The third scenario was implemented considering transaction electrical, heating, and cooling energy carriers with the energy partners' smart buildings through electrical, district heating, and cooling networks, respectively.

Tables 8 and 9 present the optimal capacity, allocation, and characteristics of facilities for different scenarios.

For the first scenario, the cooling and heating loads were supplied by compression chillers and boilers, respectively. The installed capacity of compression chillers was 39000 kW for the fifth year of the planning horizon. No CHPs and absorption chillers were installed in this scenario. Further, the installed capacity of boilers for the fifth year of the planning horizon was 35000 kW. The maximum capacity of the photovoltaic systems was installed by the optimization process in the first year of the planning horizon, which was 14500 kW. Further, the maximum capacity of electrical energy storage systems (7100 kW) was installed for the first year of the planning horizon. The installed capacity of the wind turbines was 430.5 kW. Finally, no thermal and cooling storage facilities were installed.

For the second scenario, the optimization process installed the maximum capacity of CHPs (3199 kW). Same to the first scenario outputs, the process installed the maximum capacity of the photovoltaic system and wind turbine system for the first year of the planning horizon of the second scenario. By comparing the installed capacity of the compression chiller for the first and second scenarios, it can be
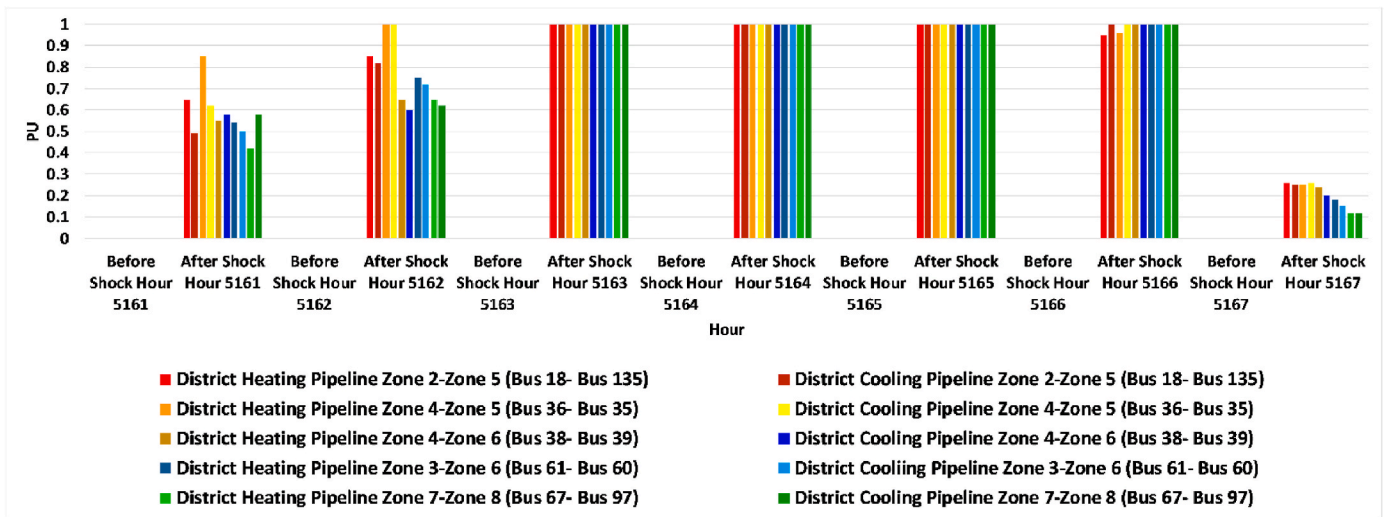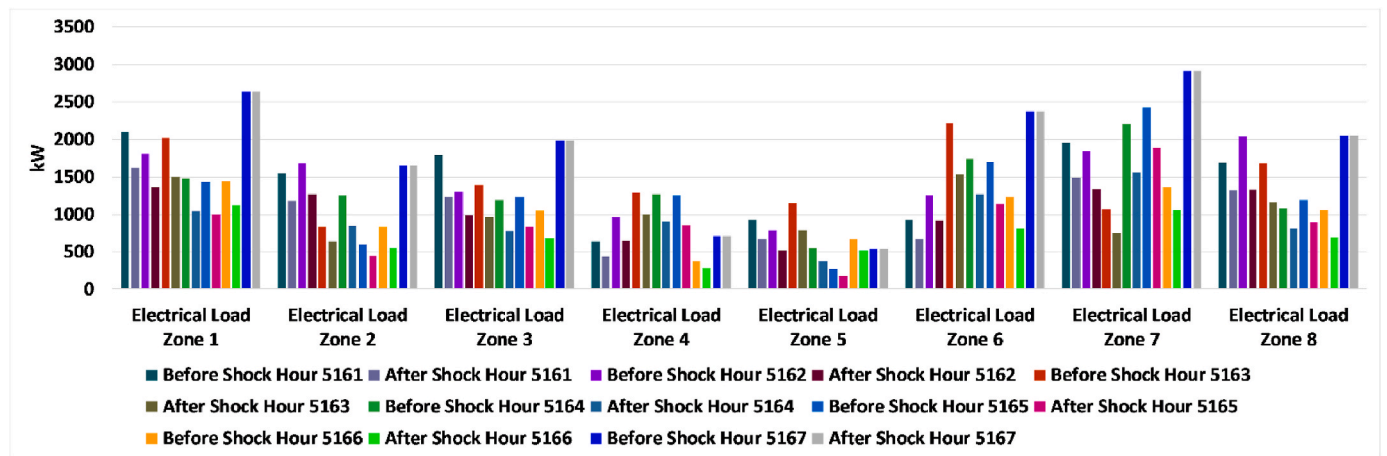
Fig. 23. The heating and cooling energy carriers flow in district heating and cooling pipelines of different zones before and after external shock.

(a)
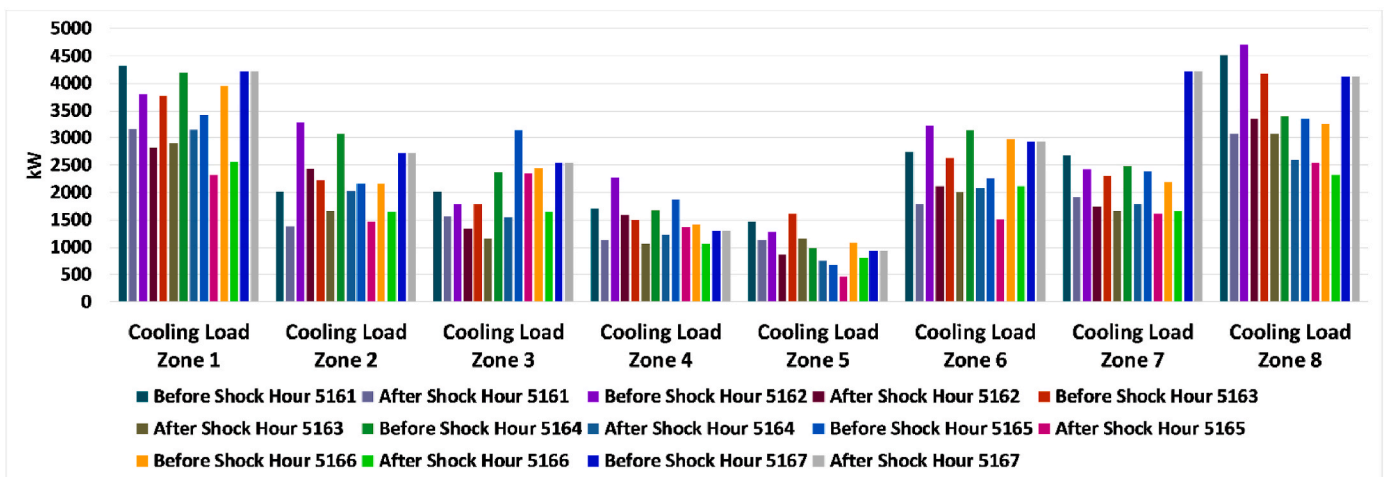
(b)

Fig. 24. (a) The direct load control process for the electrical loads, (b) The direct load control process for the cooling loads.

concluded that the installed capacity of compression chillers for the second scenario was reduced by about 41.02% concerning the first scenario. Further, the installed capacity of distributed generation facilities was reduced by about 29.62% concerning the first scenario. The

(a)

(b)

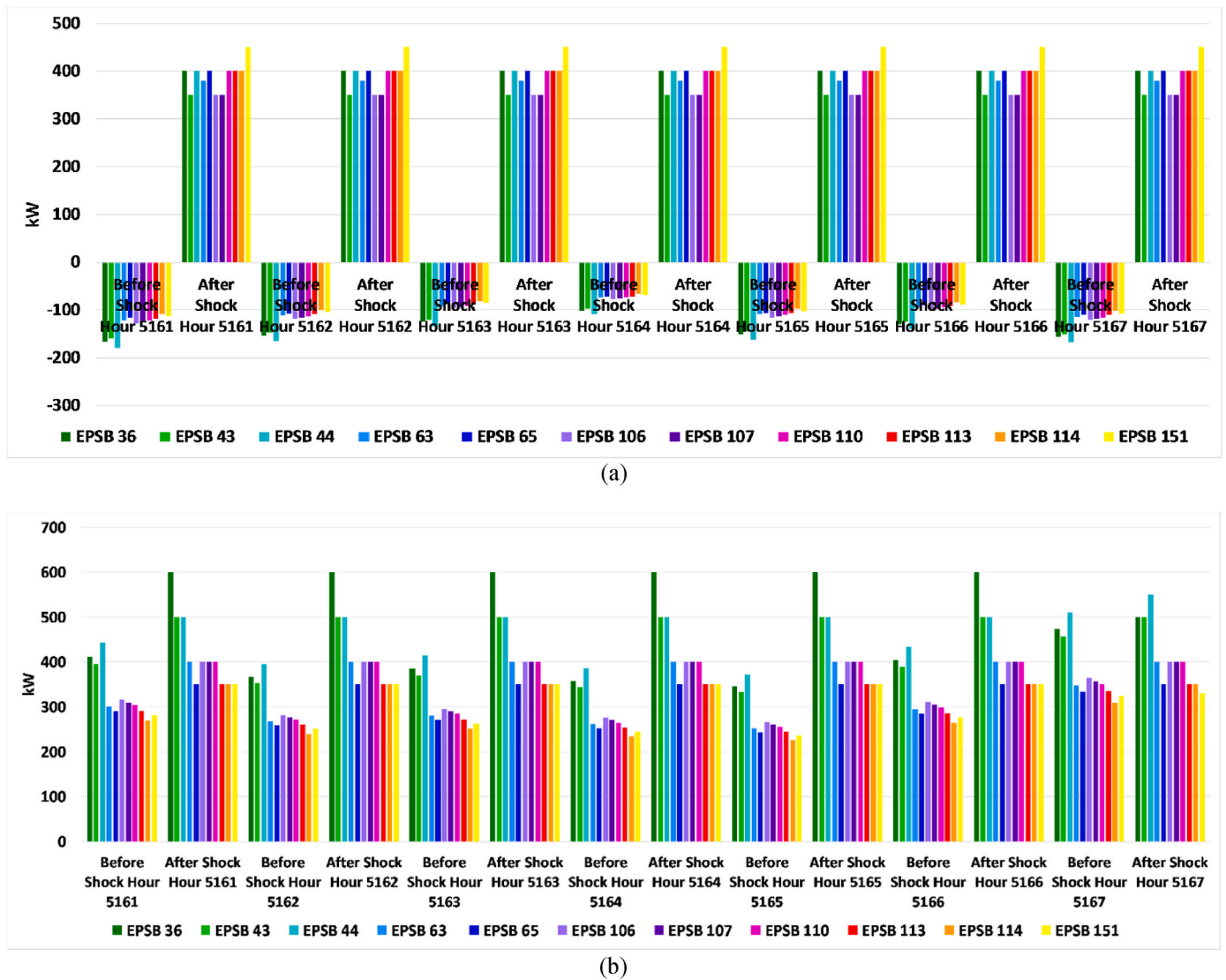**Fig. 25.** (a) The energy partner smart buildings electrical energy injection to the system after external shock, (b) The energy partner smart buildings cooling energy injection to the system after external shock.

Table 10
The OSESP algorithm computation time, the number of variables, and iterations.

Continuous variables	Discrete variables	Total equations	CPU time (sec)	Number of four-stage OSESP iterations
11126757	169047	17933781	10852	2

algorithm installed 3800 kW, 35000 kW, and 4650 kW distributed generation facilities, boilers, and absorption chillers for the final year of the planning horizon, respectively. Further, the installed capacity of compression chillers and electrical energy storages were 39000 kW and 7100 kW for the final year of the planning horizon, respectively. Thus, both the first and second scenarios installed the same value of capacity for the compression chillers and electrical energy storages in the final year of the planning process.

For the third and fourth scenarios, the optimization process installed the maximum capacity of the photovoltaic systems and wind turbine systems for the first year of the planning horizon, which were 14500 kW and 430.5 kW, respectively. Further, the installed capacity of distributed generation facilities for the third scenario was 2250 kW for the fifth year, which was reduced by about 40.79% concerning the second

scenario. The installed capacity of combined heat and power generation facilities for the third and fourth scenarios were 3199 kW and 2531 kW for the fifth year of planning, respectively. Thus, the fourth scenario's installed capacity of combined heat and power facilities was reduced by about 20.88% concerning the third scenario. The installed capacities of boilers, absorption chillers, and compression chillers for the fourth scenario and fifth year were 23000 kW, 3450 kW, and 28500 kW, respectively. By comparing the value of installed capacities of boilers, absorption chillers, and compression chillers for the fourth scenario, it can be concluded that the capacities of these facilities were reduced by about 34.28%, 25.80%, and 26.92%, respectively concerning the second scenario. However, the installed capacity of CSSs and TSSs were 40 MWh and 34 MWh, respectively for the fourth scenario and final year.

The final topology of the system for the fourth scenario and final planning year is presented in Fig. 6. The district heating and cooling networks topologies are the same as the electrical system topology for the final year of planning based on the fact that the urban energy tunnels were constructed based on the common routes of multi-carrier energy networks.

Fig. 7 (a) and Fig. 7 (b) present the submitted values of EPSBs' active power and the accepted values of EPSBs' active power for the third scenario and the final year of the planning horizon, respectively. The

aggregated values of submitted and accepted values of EPSBs' active power were 10608383 kWh and 9939030 kWh, respectively. Thus, the accepted active power bids of EPSBs were about 93.69% concerning the aggregated EPSBs' active power bids. Further, the maximum and average values of submitted active power bids of energy partner smart buildings were 8319.191 kW and 1211.003 kW, respectively. However, the maximum and average values of accepted active power bids of energy partner smart buildings were 7231.825 kW and 1134.592 kW, respectively. The aggregated yearly electricity consumption of the system was about 109555283 kWh for the final planning year.

Fig. 7 (c) and Fig. 7 (d) present the submitted values of EPSBs' reactive power and the accepted values of EPSBs' reactive power for the third scenario and the final year of the planning horizon, respectively. The maximum and average values of submitted reactive power bids of energy partner smart buildings were 3036.474 kVAr and 442.012 kVAr, respectively. Further, the maximum and average values of accepted reactive power bids of energy partner smart buildings were 2639.521 kVAr and 414.122 kVAr, respectively. The accepted reactive power bids of EPSBs were about 93.72% concerning the aggregated EPSBs reactive power bids.

Finally, Fig. 7(e) and Fig. 7 (f) present the submitted values of EPSBs' spinning reserve and the accepted values of EPSBs' spinning reserve for the third scenario and the final year of the planning horizon, respectively. As shown in Fig. 7 (e), the maximum and average values of submitted spinning reserve bids of energy partner smart buildings were 10260.231 kW and 2790.619 kW, respectively. Further, as shown in Fig. 7 (f), the maximum and average values of accepted spinning reserve bids of energy partner smart buildings were 8919.161 kW and 2417.665 kW, respectively.

Fig. 8 (a), (b), and (c) show the estimated values of the active power of distributed generation for the final year of planning and the third scenario. The aggregated electrical energy generation of distributed generation facilities was about 6484038 kWh for the final year. The average value of active power generation of distributed generation facilities was about 61.68 kWh for the final year of the planning horizon. The aggregated electrical energy generation of distributed generation facilities was about 8.04% of the total electrical demand of the system.

Fig. 9 depicts the estimated values of heating energy generation of boilers for the third scenario and the final planning year. The aggregated heating energy generation of boilers was about 42270518 kWh. Thus, the boilers supplied the heating energy by about 51.89%. The average value of heating generation of boilers was about 4825.40 kW for the final planning year. The boilers followed the heating load and supplied the residual heating loads that were not supplied by the combined heating and power facilities. Further, the boilers were continuously committed for the 2621–6944 h.

Fig. 10 (a) and Fig. 10 (b) present the cooling energy generation of absorption chillers and compression chillers for the final year of planning and the third scenario, respectively. The aggregated cooling energy generations of absorption and compression chillers for the final planning year were about 27633900 kWh and 50336233 kWh, respectively. Thus, the absorption and compression chillers supplied the cooling loads by about 35.44% and 64.56%, respectively. The average value of cooling energy generations of absorption and compression chillers were about 394.32 kWh and 718.34 kWh, respectively. The absorption chillers were fully committed and the compression chillers tracked the cooling loads.

The aggregated electrical generation of CHPs was about 28023240 kWh for the final year of the planning horizon, which was 25.57% of the electrical energy consumption of the system. Fig. 11 presents the electrical energy transactions with the upward electricity market for the final year of planning and the third scenario. The aggregated electricity transactions were about −69702740 kWh for the final year of planning. The average value of electricity transactions was about −7956.9 kWh for the final planning year. The maximum and minimum values of electricity transactions were 8155.8 kWh and −25599.1 kWh, respectively.

Fig. 12 (a) and Fig. 12 (b) show the submitted values of EPSBs' active power and the accepted values of EPSBs' active power for the fourth scenario and final year of the planning process, respectively. The aggregated values of submitted and accepted values of EPSBs' active power were 7858414 kWh and 7362583 kWh, respectively. The accepted active power bids of EPSBs were about 93.8% concerning the aggregated EPSBs' active power bids. Further, by comparing the third and fourth scenarios' results, it can be concluded that the submitted values of EPSBs' active power and the accepted values of EPSBs' active power were reduced by about 74% and 74.15%, respectively based on the fact that the EPSBs transacted heating and cooling energy carriers with the distribution system. The maximum and average values of submitted active power bids of energy partner smart buildings were 6265.87 kW and 897.1 kW, respectively. However, the maximum and average values of accepted active power bids of energy partner smart buildings were 6040.76 kW and 840.47 kW, respectively.

Fig. 12 (c) and Fig. 12 (d) depict the submitted values of EPSBs' reactive power and the accepted values of EPSBs' reactive power for the fourth scenario and the final year of the planning horizon, respectively.

The aggregated values of submitted and accepted values of EPSBs' reactive power were 2865964 kVArh and 2685134 kVArh, respectively. The maximum values of submitted and accepted reactive power bids of energy partner smart buildings were 2285.16 kVAr and 2203.1 kVAr, respectively. Further, the average values of submitted and accepted reactive power bids of energy partner smart buildings were 327.16 kVAr and 306.52 kVAr, respectively.

Finally, Fig. 12(e) and Fig. 12 (f) show the submitted values of EPSBs' spinning reserve and the accepted values of EPSBs' spinning reserve for the fourth scenario and the final year of the planning horizon, respectively. As shown in Fig. 12 (e), the maximum and average values of submitted spinning reserve bids of energy partner smart buildings were 6955.12 kW and 1855.2 kW, respectively. Further, as shown in Fig. 12 (f), the maximum and average values of accepted spinning reserve bids of energy partner smart buildings were 6705.24 kW and 1607.85 kW, respectively.

By comparing the value of bidding of energy partner smart buildings for the third scenario and fourth scenarios, it can be concluded that the energy partner buildings reduced the average values of their active power, reactive power, and spinning reserve bids by about 74%, 74.12%, and 66.55%, respectively. This reduction occurred based on the fact the EPSBs simultaneously injected electricity, heating, and cooling energy carriers into the SMCES networks, which reduced the capabilities of EPSBs' DERs to inject multi-carriers energy into the system concerning the case that the EPSBs only transacted electricity with the system.

The aggregated annual injected heating and cooling energy carriers of energy partner smart buildings were about 10704634 kWh and 29919626 kWh, respectively. The average values of the injected heating and cooling energy carriers of energy partner smart buildings were about 1221.991 kWh and 3415.482 kWh, respectively.

Fig. 13 (a), (b), and (c) present the estimated values of the active power generation of DGs for the final year of planning and the fourth scenario. The aggregated electrical energy generation of distributed generation facilities was about 11342384 kWh for the final planning year. The average value of active power generation of distributed generation facilities was about 92.47 kWh for the final planning year. By comparing the value of energy generation of distributed generation facilities for the third and fourth scenarios, it can be concluded that the electricity generation of these facilities increased by about 76.16% for the fourth scenario.

Fig. 14 depicts the estimated values of heating energy generation of boilers for the fourth scenario and the final planning year. The aggregated heating energy generation of boilers was about 39725199 kWh for the final planning year. The average value of heating generation of boilers was about 4534.84 kW for the final planning year. The boilers were continuously committed for 2621–6944 h. The heating energy generation of boilers was reduced by about 6.02% concerning the third

scenario's outputs.

Fig. 15 presents the electricity generation of combined heat and power generation facilities for the final year of planning and the fourth scenario. The CHPs were fully committed and the estimated electrical energy generation of these facilities was about 22171560 kWh for the final year of the planning horizon.

Fig. 16 (a) and (b) present the cooling energy generation of absorption chillers and compression chillers for the final year of the planning and the fourth scenario, respectively. The aggregated cooling energy generations of absorption and compression chillers for the final planning year were about 20494300 kWh and 27556207 kWh, respectively. The average value of cooling energy generations of absorption and compression chillers were about 292.44 kWh and 890.21 kWh, respectively. By comparing the value of cooling energy generation of absorption and compression chillers for the third and fourth scenarios, it can be concluded that the cooling energy generation of absorption and compression chillers reduced by about 25.83% and 45.25%, respectively.

Fig. 17 presents the electricity transactions of PHEV parking lots with the energy system for the final year of planning and the fourth scenario. The aggregated transacted electrical energy of PHEVs with the energy system was about 10137421 kWh and the average value of the transacted energy was about 1157.239 kWh.

Fig. 18 presents the electrical energy transactions with the upward electricity market for the final year of planning and the fourth scenario. The aggregated electricity transaction was about −64717405 kWh for the final year of planning. The average value of electricity transactions was about −7387.83 kW for the final planning year. The maximum and minimum values of electricity transactions were 7065.04 kWh and −23644 kWh, respectively. It can be concluded that the imported electricity from the upward market was reduced by about 6.29% concerning the third case based on the fact that the SMCES delivered more electricity to the upward network to gain more profit.

Fig. 19 (a) presents the aggregated operational and interruption costs of the system for the 48 worst-case external shocks for the fourth scenario. The maximum value of the aggregated operational and interruption costs for the fourth scenario took the value 2963940 MUs for external shock = 48 and hour = 903. The minimum value of the aggregated operational and interruption costs for the fourth scenario took the value of 1.1288 MUs for the external shock = 29 and hour = 1721.

Fig. 19 (b) depicts the aggregated operational and interruption costs of the system for the 48 worst-case external shocks and the first scenario. The maximum value of the aggregated operational and interruption costs for the first scenario took the value 142820578 MUs for the external shock = 48 and hour = 86. However, the maximum value of the aggregated operational and interruption costs for the fourth scenario was about 1293097 MUs for the external shock = 48 h = 86. Thus, the proposed method reduced the aggregated operational and interruption costs of the system by about 99.09% for the external shock = 48 and hour = 86. Further, by comparing Fig. 19 (a) and Fig. 19 (b), it can be concluded that the proposed method reduced the aggregated operational and interruption costs by about 24.34% for the 48 worst-case external shocks.

Fig. 20 (a) presents the self-healing performance index for the first scenario and the 48 worst-case external shocks. The average value of SPI was about 84.32 for the first scenario, which indicated that the designed system was completely vulnerable to the considered external shocks. Fig. 20 (b) depicts the self-healing performance index for the designed system of the second scenario and the 48 worst-case external shocks. The average value of SPI was about 136.5, which indicated that the designed system of the second scenario was vulnerable to the considered external shocks. Fig. 20 (c) shows the SPI for the district heating and cooling designed systems of the third scenario and the 48 worst-case external shocks. The value of SPI for the electrical designed system tended to the infinity. However, the district heating and cooling systems of the third

scenario were completely vulnerable to the considered external shocks. The average value of SPI for the district heating and cooling systems was about 81.69.

However, the self-healing performance index for electrical, heating, and cooling systems tended to the infinity for all of the 48 external shocks for the fourth scenario.

Fig. 21 depicts the final investment and energy not supplied costs, electricity generation costs, and operating costs for the considered scenarios at the horizon year of planning. According to Fig. 21, the implementation of the proposed method reduced the aggregated costs of the system for the fourth scenario by about 49.92% concerning the first scenario costs. Further, the proposed method reduced the operating costs and energy not supplied costs by about 54.01% and 93.64%, respectively.

The external shock 48 was one of the worst-case scenarios of external shocks and the following facilities were out of service for 4 h for this shock.

- Four lines, one CHP, and absorption chiller of the fifth zone (line 47–48, line 47–49, line 49–50, line 44–47, CHP bus 44, absorption chiller bus 44),
- Three lines, one CHP, and absorption chiller of the sixth zone (line 50–51, line 51–151, line 64–65, CHP bus 64, absorption chiller bus 64),
- Four lines, one CHP, and absorption and compression chillers of the eighth zone (line 110–111, line 110–112, line 112–113, line 108–109, CHP bus 112, absorption chiller bus 112, compression chiller bus 108).

The condition of the SMCES for this credible external shock is explored in the next paragraphs. The fourth stage optimization process was carried out for the described external shock and the optimal dispatch of system resources, electrical system topology, and status of control valves were determined.

Fig. 22 (a), (b), (c), (d) present the optimal dispatch values of DGs, CSSs and TSSs, ESSs, and PHEVs, respectively. The distributed generation units of the shock-affected zones were fully committed. According to Fig. 22 (b), the CSSs and TSSs compensated for the mismatch of cooling and heating generations and consumptions in the shock-affected zones. As shown in Fig. 22 (c) and Fig. 22 (d), the ESSs and PHEV parking lots were committed to supply the electrical loads of the shock-affected zones.

Fig. 23 shows the heating and cooling energy carriers flow in district heating and cooling pipelines of different zones before and after external shock. The control valves of district heating and cooling pipelines were opened to transfer the heating and cooling energy carriers to the shock-affected zones.

Fig. 24 (a) and (b) depict the direct load control process for the electrical loads and cooling loads, respectively. As shown in Fig. 24 (a), the maximum value of electrical load control was about 29.36% for the 5164th hour, and the aggregated electrical load of the system reduced from 10783.35 kW to 7616.869 kW. The average value of the electrical load direct load control was about 28.13% of total controllable loads for 4 h after the external shock. According to Fig. 24 (b), the maximum value of cooling load control was about 29.58% for the 5164th hour, and the aggregated cooling load of the system reduced from 21487.94 kW to 15131.89 kW. The average value of the cooling load direct load control was about 28.70% of total controllable loads for 4 h after the external shock.

Fig. 25 (a) and (b) present the energy partner smart buildings' electrical and cooling energy injection to the system after the external shock, respectively. The aggregated values of electrical energy injection of energy partner smart buildings were −8613.27 kWh and 29960 kWh before and after the external shock, respectively. Further, the aggregated values of cooling energy injection of energy partner smart buildings were 24083.8 kWh and 32130 kWh before and after the external shock,

respectively. Thus, the energy partner smart buildings injected electrical and cooling energy carriers into the SMCES to mitigate the impacts of the external shock. It can be concluded that the energy partner smart buildings' contributions may highly reduce the investment costs, energy not supplied costs, and operating costs of the SMCES and increase the self-healing performance index of the system. Thus, the energy system operator should consider the available energy partner smart buildings resources in the planning processes.

Table 10 shows the number of continuous and discrete variables, the number of equations, and OSESP iterations for the final planning year. The simulation was carried out on a PC (Intel Core i7-13700 processor, 128 GB memory, DDR4 3200 MT). The number of equations for the test system was 17933781, which indicated the curse of dimensionality. The maximum CPU time required to solve the fourth scenario was about 10852 s.

In conclusion, the proposed optimization algorithm successfully considered the impacts of the contributions of smart buildings in the planning practices of the energy system. Further, the proposed model utilized the self-healing performance index to explore the impacts of the contributions of the smart buildings on the system costs. The current research can be improved by considering the transition states between smart buildings operating modes and modeling the dynamic behavior of smart buildings. Further, the OSESP process should be updated based on regulatory policies that may change energy prices, investment alternatives, energy carriers' market conditions, and technological advancements. As a limitation of this work, it should be noted that the curse of dimensionality is a major problem, and other optimization processes should be examined to solve the proposed problem. The authors are working on the modeling and optimization of other multi-carrier energy resources in the OSESP process.

5. Conclusion

This paper introduced an iterative four-stage optimization algorithm for optimal planning of the multi-carrier energy system considering smart buildings and parking lots commitment scenarios. The proposed algorithm utilized the self-healing performance index to assess the level of self-healing of the multi-carrier energy system in the worst-case conditions. In the first stage, the location, capacity, and specifications of energy system facilities were determined. In the second stage, the contribution scenarios of smart buildings and parking lots were explored. In the third stage, the operational scheduling of the system resources in normal conditions was determined. Finally, in the fourth stage, the optimal scheduling of system resources, the status of electrical switches, and control valves were determined for external shock conditions. The introduced algorithm was assessed for the 123-bus test system and different scenarios were considered. The proposed method reduced the aggregated operational and interruption costs of the system by about 99.09% for the worst-case external shock concerning the custom planning exercise.

Credit authorship contribution statement

M.S. Nazar: Conceptualization, Methodology, Supervision.
P. Jafarpour: Investigation, Data curation, Writing – original draft.
M. Shafie-khah: Formal analysis, Validation.
J.P.S. Catalão: Visualization, Writing – review & editing.

Declaration of competing interest

The authors declare that they have no known competing financial interests or personal relationships that could have appeared to influence the work reported in this paper.

Data availability

The data that has been used is confidential.

References

[1] Firouzi M, Setayesh Nazar M, Shafie-khah MR, Catalão JPS. Integrated framework for modeling the interactions of plug-in hybrid electric vehicles aggregators, parking lots and distributed generation facilities in electricity markets. Appl Energy 2023;334:120703.
[2] Diahovchenko Illia M, Kandaperumal Gowtham, Srivastava Anurag K. Enabling resiliency using microgrids with dynamic boundaries. Elec Power Syst Res 2023; 221:109460.
[3] Kagan Candan Alper, Rifat Boynuegri Ali, Onat Nevzat. Home energy management system for enhancing grid resiliency in post-disaster recovery period using Electric Vehicle. Sustainable Energy, Grids and Networks 2023;34:101015.
[4] Zakernezhad H, Setayesh Nazar M, Shafie-khah MR, Catalão JPS. Multi-level optimization framework for resilient distribution system expansion planning with distributed energy resources. Energy 2021;214:118807.
[5] Borghei M, Ghasemi M. Optimal planning of microgrids for resilient distribution networks. Int J Electr Power Energy Syst 2021;128:106682.
[6] Wu D, Ma X, Huang S, Fu T, Balducci P. Stochastic optimal sizing of distributed energy resources for a cost effective and resilient microgrid. Energy 2020;198: 117284.
[7] Mousavizadeh S, Ghanizadeh Bolandi T, Haghifam MR. Resiliency analysis of electric distribution networks: a new approach based. Int J Electr Power Energy Syst 2020;117:105669.
[8] Bessani M, Massignan J, Fanucchi R, Camillo M, London J, Delbem A, Maciel C. Probabilistic assessment of power distribution systems resilience under extreme weather. IEEE Syst J 2019;13(2):1747–56.
[9] Mishra S, Bordin C, Tomasgard A, Palua A. A multi-agent system approach for optimal microgrid expansion planning. Int J Electr Power Energy Syst 2019;109: 696–709.
[10] Gilani MA, Kazemi A, Ghasemi M. Distribution system resilience enhancement by microgrid formation considering distributed energy resources. Energy 2019;191: 116442.
[11] Zare-Bahramabadi M, Abbaspour A, Fotuhi-Firuzabad M, Moeini-Aghtaie M. Resilience-based framework for switch placement problem in power distribution systems. IET Gener Transm Distrib 2018;12(5):1223–30.
[12] Lin Y, Bie Z. Tri-stage optimal hardening plan for a resilient distribution system considering reconfiguration and DG islanding. Appl Energy 2018;210:1266–79.
[13] Yuan W, Wang J, Qiu F, Chen C, Kang C, Zeng B. Robust optimization-based resilient distribution network planning against natural disasters. IEEE Trans Smart Grid 2016;7:2817–26.
[14] Arefifar SA, Mohamed YA, El-Fouly TH. Comprehensive operational planning framework for self-healing control actions in smart distribution grids. IEEE Trans Power Syst 2013;28:4192–200.
[15] Qaeini S, Setayesh Nazar M, Varasteh F, Shafie-khah MR, Catalão JPS. Combined heat and power units and network expansion planning considering distributed energy resources and demand response programs. Energy Convers Manag 2020; 211:112776.
[16] Varasteh F, Setayesh Nazar M, Heidari A, Shafie-khah M, Catalão JPS. Distributed energy resource and network expansion planning of a CCHP based active microgrid considering demand response programs. Energy 2019;172:79–105.
[17] Zheng Xuyue, Wu Guoce, Qiu Yuwei, Zhan Xiangyan, Shah Nilay, Ning Li, Zhao Yingru. A MINLP multi-objective optimization model for operational planning of a case study CCHP system in urban China. Appl Energy 2018;210: 1126–40.
[18] Li Zelin, An Qingsong, Zhao Jun, Deng Shuai, Kang Ligai, Wang Yongzhen. Analysis of system optimization for CCHP system with different feed-in tariff policies. Energy Proc 2017;105:2484–91.
[19] Ju Liwei, Tan Zhongfu, Li Huanhuan, Tan Qingkun, Yu Xiaobao, Song Xiaohua. Multi-objective operation optimization and evaluation model for CCHP and renewable energy based hybrid energy system driven by distributed energy resources in China. Energy 2016;111:322–40.
[20] Li Miao, Mu Hailin, Li Nan, Ma Baoyu. Optimal design and operation strategy for integrated evaluation of CCHP (combined cooling heating and power) system. Energy 2016;99:202–20.
[21] Hadi Shaban Boloukat M, Akbari Foroud A. Stochastic-based resource expansion planning for a grid-connected microgrid using interval linear programming. Energy 2016;113:776–87.
[22] Hemmati R, Saboori H, Siano P. Coordinated short-term scheduling and long-term expansion planning in microgrids incorporating renewable energy resources and energy storage systems. Energy 2017;134:699–708.
[23] Weber C, Shah N. Optimization based design of a district energy system for an eco-town in the United Kingdom. Energy 2011;36:1292–308.
[24] Bracco S, Gabriele D, Silvia S. Economic and environmental optimization model for the design and the operation of a combined heat and power distributed generation system in an urban area. Energy 2013;55:1014–24.
[25] Mehleri ED, Sarimveis H, Markatos NC, Papageorgiou LG. Optimal design and operation of distributed energy systems: application to Greek residential sector. Renew Energy 2013;51:331–42.

[26] Alilou M, Tousi B, Shayeghi H. Home energy management in a residential smart micro grid under stochastic penetration of solar panels and electric vehicles. Sol Energy 2020;212:6–18.

[27] Buffaa S, Cozzini M, D'Antoni M, Baratieri M, Fedrizzi R. 5th generation district heating and cooling systems: a review of existing cases in Europe. Renew Sustain Energy Rev 2019;104:504–22.

[28] Bostan A, Setayesh Nazar M, Shafie-khah MR, Catalão JPS. An integrated optimization framework for combined heat and power units, distributed generation and plug-in electric vehicles. Energy 2020;202:117789.

[29] Eichhorn A, Heitsch H, Römisch W. "Stochastic optimization of electricity portfolios: scenario tree modeling and risk management", *Handbook of power systems* II. Berlin, Heidelberg: Springer; 2010.

[30] Heitsch H, Römisch W. Scenario reduction algorithms in stochastic programming. Comput Optim Appl 2003;24:187–206.

[31] Lobato FS, Steffen Jr V. Multi-objective optimization problems concepts and self-adaptive parameters with mathematical and engineering applications. Springer Press; 2017.

[32] Sanaye S, Khakpaay N. Simultaneous use of MRM (maximum rectangle method) and optimization methods in determining nominal capacity of gas engines in CCHP (combined cooling, heating and power) systems. Energy 2014;72:145–58.

[33] Wind turbine data sheets. URL: https://www.renugen.co.uk/content/medium_wind_turbine_brochures/50_030_001_C_MANUAL_windspot_3.5_y_1.5_Manual.pdf.

[34] Photovoltaic costs and prices sheets, URL:https://www.nrel.gov/docs/fy15osti/64746.pdf.

[35] Chillers data sheets, URL:www.carrier.com/commercial/en/us/products/chillers-components/chillers.